A MECHANISTIC STUDY OF ALCOHOL ADDITION TO

1,1-DIPHENYLSILENE

A MECHANISTIC STUDY OF ALCOHOL ADDITION TO 1,1-DIPHENYLSILENE

by

JO-ANN HELENA BANISCH, B.Sc.

A Thesis

Submitted to the School of Graduate Studies

in Partial Fulfilment of the Requirements

for the Degree

Master of Science

McMaster University

MASTER OF SCIENCE (1995) **McMASTER UNIVERSITY**

(Chemistry) **Hamilton, Ontario**

TITLE: **A Mechanistic Study of Alcohol Addition to 1,1-Diphenylsilene**

AUTHOR: Jo-Ann Helena Banisch, B.Sc. (McMaster University)

SUPERVISOR: Professor William J. Leigh

NUMBER OF PAGES: 95

ABSTRACT

The photochemistry of 1,1-diphenylsilacyclobutane has been studied by steady-state and nanosecond laser flash photolysis *(NLFP)* techniques in order to investigate the mechanism of reaction of a transient silene with alcohols. *NLFP* of 1,1-diphenylsilacyclobutane (**I**) in acetonitrile solution at 325 nm results in the formation of 1,1-diphenylsilene (**II**) derived from excited-state [2+2]-cycloreversion of the silacyclobutane. The transient has a lifetime of 100 ns - 1.2 μs in acetonitrile solution at room temperature, depending on the presence of water in the solvent. Steady-state photolysis in the presence of various σ-bonded nucleophiles such as methanol results in the generation of a single product in each case, consistent with addition of the nucleophile to the silene (**II**). Absolute rate constants (k_q) have been determined by *NLFP* techniques for reactions of the silene with water, methanol, ethanol, *tert*-butyl alcohol, 2-propanol, 2,2,2-trifluoroethanol, 1,1,1,3,3,3-hexafluoroisopropanol, and glacial acetic acid. The rate constants (k_q) illustrate the following characteristics: linear quenching plots characteristic of second order kinetics, observation of small but detectable deuterium kinetic isotope effects, and an inverse Arrhenius temperature dependence. Two possible mechanisms will be discussed based on these results.

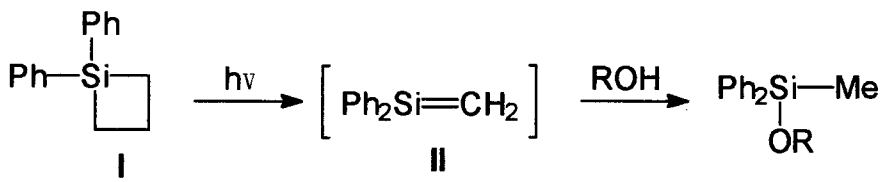

TABLE OF CONTENTS

LIST OF SCHEMES

LIST OF FIGURES

2.6 (b) *Time-resolved UV Absorption Spectrum*: Recorded 125-485 ns after 248 nm nanosecond laser lash photolysis of an oxygen-saturated 3.1×10^{-3} M solution of **6** in acetonitrile (MeCN) at 22.8 °C.

2.7 (a) *Transient Decay Trace*: Recorded at 325 nm from 248 nm nanosecond laser flash photolysis of an oxygenated 3.1×10^{-3} M solution of **6** in isooctane at 21.7 °C.

(b) *Time-resolved UV Absorption Spectrum:* Recorded 1.6-4.7 μs after 248 nm nanosecond laser lash photolysis of an oxygen-saturated 3.1×10^{-3} M solution of **6** in isooctane at 21.7 °C.

2.8 (a) *Transient Decay Trace*: Recorded at 325 nm from 248 nm nanosecond laser flash photolysis of an oxygenated 3.1×10^{-3} M solution of **6** in hexane at 22.4 °C.

(b) *Time-resolved UV Absorption Spectrum*: Recorded 176-509 ns after 248 nm nanosecond laser lash photolysis of an oxygen-saturated 3.1×10^{-3} M solution of **6** in hexane at 22.4 °C.

2.9 (a) *Transient Decay Trace:* Recorded at 325 nm from 248 nm nanosecond laser flash photolysis of an oxygenated 3.1×10^{-3} M solution of **6** in tetrahydrofuran at 21.6 °C.

(b) *Time-resolved UV Absorption Spectrum*: Recorded 0.8-1.4 μs after 248 nm nanosecond laser lash photolysis of an oxygen-saturated 3.1×10^{-3} M solution of **6** in tetrahydrofuran at 21.6 °C.

2.10 Quenching plots of k_{decay} of **7** versus quencher concentration for: Water (■) (20.7 °C) and Deuterium oxide (▲) (21.1 °C) in MeCN (Table2.4).

2.11 Quenching plots of k_{decay} of **7** versus quencher concentration for: Methanol (■) (28.9 °C) and Methanol-d (▲) (28.0 °C) in MeCN (Tables 2.5-2.6).

LIST OF TABLES

CHAPTER 1

INTRODUCTION

1.1 Reactive Silicon Intermediates

Silenes, compounds containing a Si=C bond, have been the subject of intense interest over the past two decades.[1-21] They are molecules of intrinsically low thermodynamic stability, primarily due to the poor π-bond overlap between the 3p and 2p atomic orbitals on the silicon and carbon atoms, respectively.[7,8,36] The first indication that silenes could exist at all was reported in 1967, when Gusel'nikov and Flowers[9,23] reported that pyrolysis of 1,1-dimethylsilacyclobutane (**1**) led to the formation of 1,1,3,3-disilacyclobutane (**3**) as shown in equation 1.1. The stoichiometry of the reaction and the accompanying formation of ethylene led them to suggest that the product was formed by dimerization of 1,1-dimethylsilene (**2**).

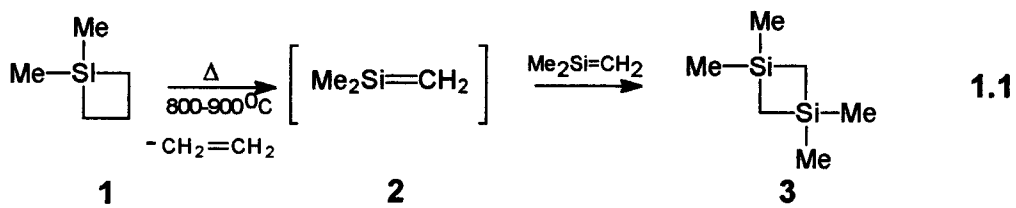

Since that time, a number of silenes have been reported, usually as reactive intermediates. Low temperature spectroscopic studies[60-62] and theoretical calculations[7,8,36] have led to a reasonably good understanding of the basic physical properties of the Si=C bond, and why it is so unstable. In recent years, several examples of stable silenes[18,20] have been reported which will be introduced shortly.

1.2 Physical Properties of Silenes

Table 1.1 compares various fundamental physical properties of ethylene ($H_2C=CH_2$), and silene ($H_2Si=CH_2$), collected from both theoretical[7,8,36] and spectroscopic studies.[60-62]

Table 1.1 Physical Properties of Ethylene and Silaethene.[a]

Property	$H_2C=CH_2$	$H_2Si=CH_2$
Bond Length (Å)	1.33	1.70
Bond Energy (kcal mol^{-1})	65	38
Dipole Moment (D)	0	0.84
Ionization Potential (eV)	-10.5	-8.8
λ_{max} (nm)	165	258

a. Data from reference 17.

The geometry of the parent silene in its ground state was calculated to be planar with a Si=C bond length of 1.70 Å,[24,25] the latter should be compared with the C=C bond length of 1.33 Å.[40] X-ray crystallographic studies of stable silenes[26,27] reveal Si=C bond distances very close to the value calculated for $H_2Si=CH_2$. The effects of substituents on the Si=C bond length of silaethene have been calculated as well.[28,29,30] Substituents that decrease the natural polarity of the $C^{\delta-}Si^{\delta+}$ bond lead to a lengthening of the Si=C.[24,29] For example, fluorine substitution on the silicon atom lengthens the Si-F bond,[36] and has

no effect on the Si=C bond. Fluorine substitution at the carbon atom shortens the C-F bond, but lengthens the Si=C bond.[28,29]

The strength of the π bond was calculated to be 38 kcal mol^{-1} for the parent silene,[24,31-33,35] which should be compared with the experimental π bond energy of 65 kcal mol^{-1} for ethylene.[40] The π bond energy represents the activation barrier for *cis-trans* isomerization. The π bond of the parent silene can be predicted to be very weak when considering the physical properties looked at thus far: longer bond length and the difference in π bond energy compared to ethylene. When creating a π-bond in a Si=C species, one must consider the two types of atomic orbitals of each atom, the silicon (3p) and carbon (2p), respectively, as shown in Figure 1.1.[4,5,35-37]

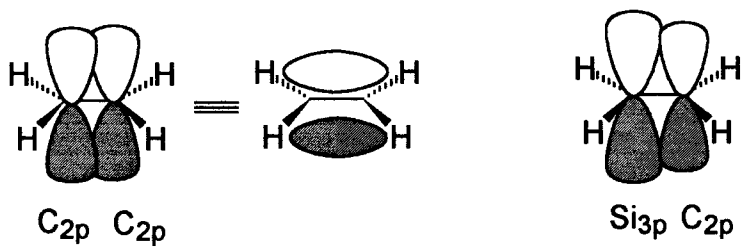

Figure 1.1 The π bond in (a) Ethylene and (b) Silaethene.

It is clear that the larger size of the silicon 3p orbital compared to that of the carbon 2p orbital results in poorer orbital overlap between the two, thereby leading to a weaker π bond in the Si=C moiety compared with the C=C.[4,5,35-37]

Another important property of chemical bonds is their polarity. Considering a pair of electrons in a covalent bond, these electrons are subject to a probability distribution that may favor one of the two atoms. Electronegativity a term used to describe the tendency of an atom to attract electrons, is extremely important in predicting the relative reactivity of molecules.[38] Qualitatively, bond polarity can be predicted by comparing the difference

in electronegativity of the bound atoms. The larger the difference, the greater the bond dipole. Comparison of the electronegativities of silicon (1.64) with carbon (2.35) indicate that the silicon atom has a partial positive-charge whereas the carbon has a negative charge.[38] The unequal distribution of electron density in covalent bonds produces a bond dipole having the units of charge times distance. Bonds with significant dipoles are described as being polar. The calculated dipole moment for ground state silaethene was reported to be 0.84 D.[24,25] This value corresponds to charges of approximately -0.6|e| on the carbon, and +0.5|e| on the silicon atom.[24,25] Thus, the calculated dipole moment indicates that the Si=C bond is polar with partial positive charge located on the silicon atom, as shown in Scheme 1.1.

Scheme 1.1 Polarization of Silenes

The ionization potential for silaethene and ethylene was experimentally found to be -8.8 eV and -10.5 eV, respectively.[39,40] The experimental measurement for silaethene was determined by photoelectron spectroscopy which measures the Ionization Potential (IP), and is in close agreement with the ab initio calculations (8.95 eV).[39] The HOMO energy (-10.5 eV) of C=C is more negative relative to the HOMO energy (-8.8 eV) of Si=C as shown in Scheme 1.2. This gives rise to a larger ΔE gap between the HOMO and LUMO for C=C, hence a stronger π-bond compared with Si=C.[39]

The position of the absorption maxima in the ultraviolet absorption spectra of silaethene and ethylene are also different. The difference can be explained by considering

the energy diagram presented in Scheme 1.2. Since the energy gap (ΔE) between the HOMO and LUMO is large, ethylene absorbs at a relatively short wavelength (high energy), *i.e.*, 165 nm.[41] Silaethene exhibits a bathochromic (red) shift in absorption to a longer wavelength, 258 nm,[42,43] which indicates that the silene absorbs at lower energies due to a smaller HOMO-LUMO gap. This is at least partially due to the higher HOMO energy in silene compared to ethylene.

Scheme 1.2 Energy Level Diagram for (π, π*) Transition

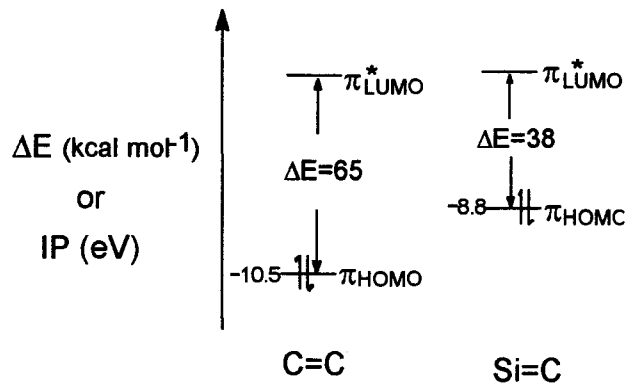

The effects of substitution on silene UV absorption spectra can be understood by considering the π system alone, since the lowest excited singlet states of silenes are thought to be of (π,π*) character.[17] Simple silenes are polarized species and as a result, the magnitudes of the orbital coefficients on silicon and carbon are quite different in the HOMO and LUMO. Now, considering the different types of substituents on the silicon atom and the effects on the energies, a π-acceptor substituent on the silicon atom should lower the energy of the LUMO (π* orbital) due to the large orbital coefficient on Si, whereas the energy of the HOMO (π orbital) should only be lowered slightly.[17] This small

HOMO-LUMO gap results in the red-shifts in the UV absorption spectra of π-acceptor substituted silenes. Likewise, a π-donor substituent on carbon should raise the HOMO without affecting the LUMO and cause a red-shift in the UV absorption.[17] A π-acceptor substituent at carbon should cause only a small red-shift in the (π, π*) transition since the LUMO will not be lowered much due to the small coefficient on carbon. These effects are summarized in Scheme 1.3.[17]

Scheme 1.3 **Effects of π-Donor and π-Acceptor Substituents on the HOMO and LUMO Energies of Silenes**

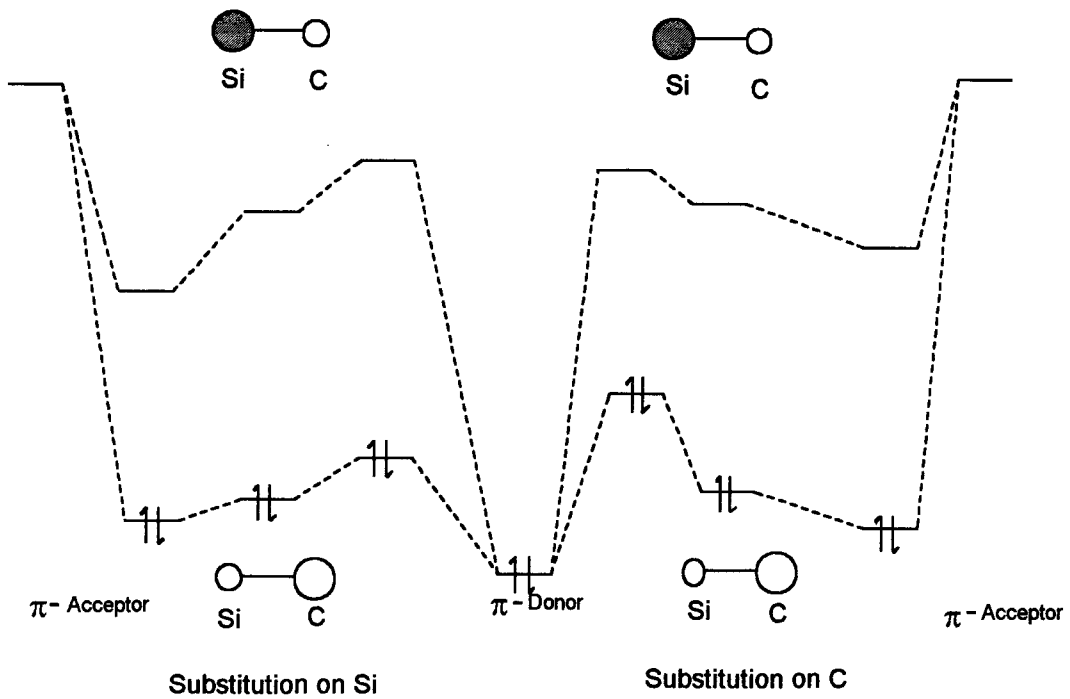

1.3 Previous Studies of Silenes

1.3.1 Chemical Trapping Experiments

For many years the existence of stable (p-p)π bonds between carbon and the group IV elements, mainly silicon and germanium, remained in doubt.[36] Despite a number of early reports proposing stable carbon-silicon double bonded compounds, only work by Gusel'nikov,[9,22,23] Barton[12,13,14] and Sommer[44,45] have placed these on a firm experimental foundation.

The most common evidence cited for the transient existence of silenes is the formation of the head-to-tail dimers, 1,3-disilacyclobutanes (**3**) (eq. 1.1) in the absence of trapping agents.[9,23]

Scheme 1.4 Common Silene Trapping Agents

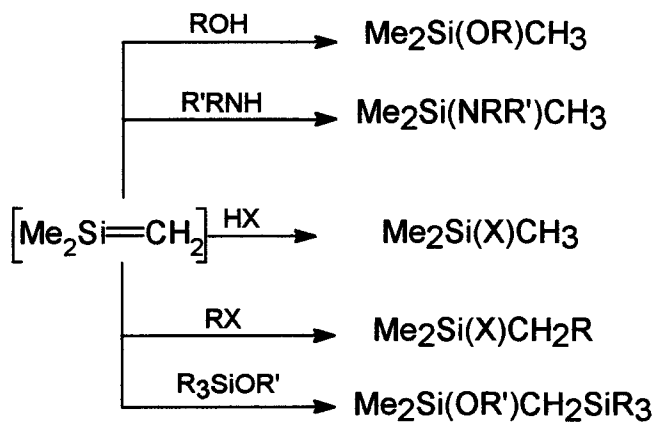

Nucleophilic σ-bonded trapping agents such as alcohols, ammonia, hydrogen halides, alkyl halides, and alkoxysilanes readily form adducts with silenes at reaction rates faster than that of dimerization as shown in Scheme 1.4.[16] The rates of these reactions are concentration dependent.

In addition to the [2+2]-cycloreversion reaction of silacyclobutanes, which was first used by Gusel'nikov and Flowers[9,23] to generate 1,1-dimethylsilene **2**, thermal [2+4]-cycloreversions have also been employed. For example, pyrolysis of 2,3-bis-(trifluoro-methyl)-7,7-dimethyl-7-silabicyclo[2.2.2]octa-2,5-diene (**4**) leads to the formation of 1,1-dimethylsilene (**2**).[42,43] This was inferred on the basis of trapping experiments with 2,3-dimethyl-1,3-butadiene, which generates **5** in competition with the formation of the head-to-tail dimer **3** (eq.1.2).[42,43]

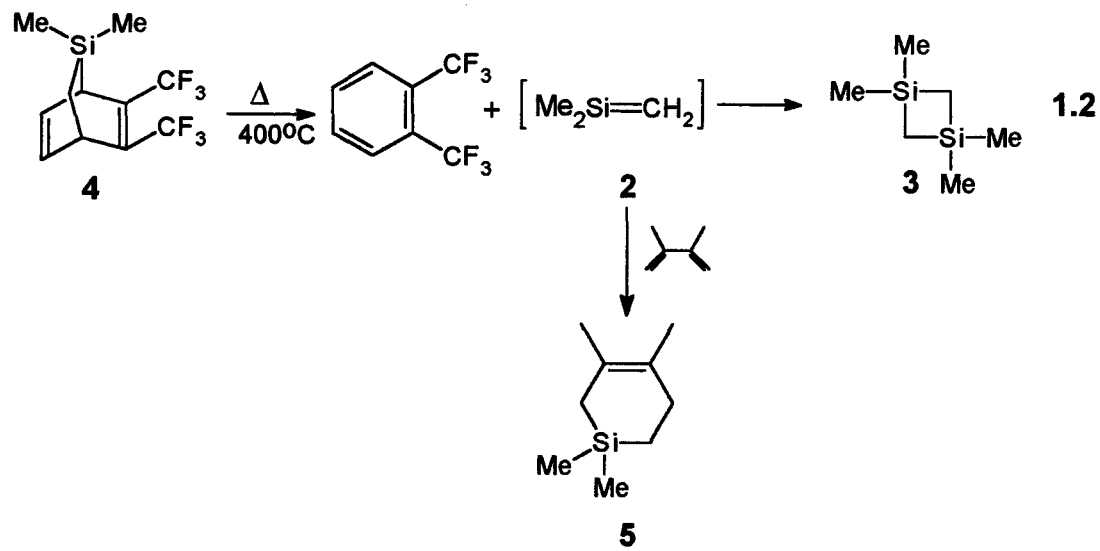

Photolysis of silacyclobutanes also leads to the formation of silenes by [2+2]-cycloreversion.[11,46] For example, liquid-phase photolysis of 1,1-diphenylsilacyclobutane (**6**) in the presence of methanol-d results in the formation of **8** consistent with the initial generation of 1,1-diphenylsilene (**7**) (eq.1.3).[48]

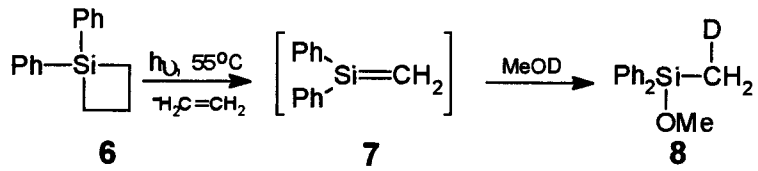

1.3

Sommer also reported that photolysis of pentaphenylmethyldisilane (**9**) in the presence of methanol-d yielded the same product (eq.1.4), consistent with the formation of 1,1-diphenylsilene (**7**) by dehydrosilylation.[49]

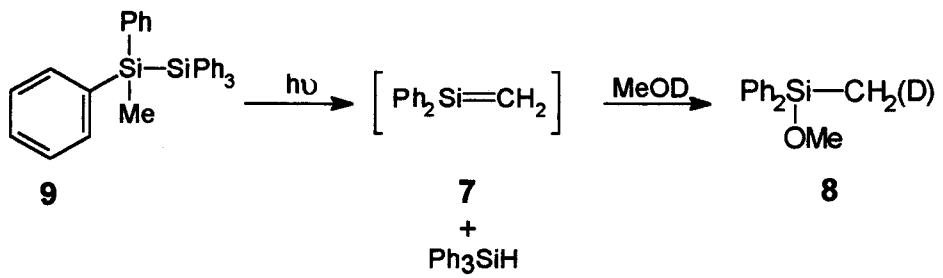

1.4

Photolysis of related aryldisilane compounds such as pentamethyl(4-tolyl)disilane in the presence of methanol has been shown to yield products consistent with methanol trapping of a highly conjugated silene formed by photochemical [1,3]-silyl migration, the [1,4]-, and [1,6]-adduct, respectively (eq.1.5).[54]

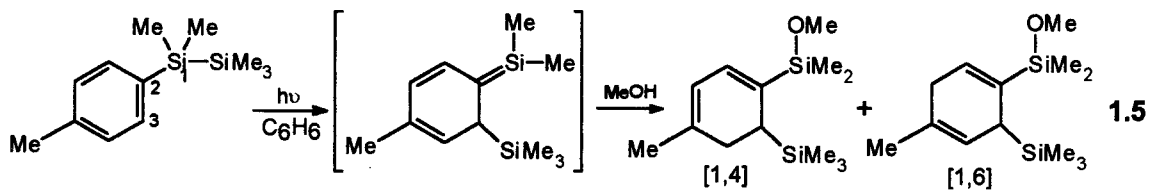

1.5

1.3.2 Low Temperature Matrix Isolation Techniques

The first direct observation of a silene was reported in 1976, using low temperature matrix isolation techniques.[60-62] Matrix isolation has played an important role in the characterization of simple silenes as well as many other types of reactive intermediates. The technique can be explained in the following manner. The vapour of the material to be examined is deposited along with an excess of inert gas, generally argon, onto a window that is at 10-20 K. Since the window is cold, the material solidifies as a mixture with the inert gas, thereby allowing very reactive species to be stable indefinitely. It is then possible to trap primary products from thermolysis as well as to trap suitable precursors necessary for subsequent photochemical conversion to highly reactive species. The primary spectroscopic techniques used to characterize these transients include infrared and ultraviolet spectroscopy.

The IR spectrum of 1,1-dimethylsilene (**2**) was reported in the late 1970's from various precursors.[63,64] One method involved the generation of the transient by the gas phase pyrolysis of 1,1-dimethylsilacyclobutane (**1**) followed by condensing the pyrolysate in an argon matrix at 10 K (eq. 1.6).[64] The IR spectrum shows three distinctive bands at 643, 825, and 1003 cm^{-1}.[63,64] These were assigned to the C-H out-of-plane bend, the vinylic Si-CH stretch, and the Si=C stretch[66], respectively[63, 64], and agreed with the calculated spectrum.[65] The IR spectrum observed for silaethene[67,68] was also found to be in agreement with the calculated spectrum.[69]

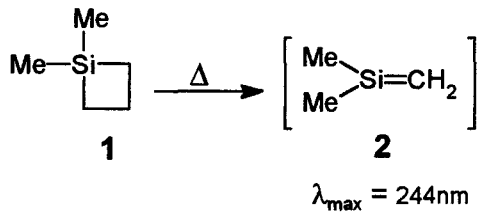

1.6

The photolysis ($\lambda > 300$ nm, Ar, 10K) of trimethylsilyldiazomethane (**15**) in an argon matrix at 10 K generates a carbene which upon further photolysis produces 1,1,2-trimethylsilene (**16**) as illustrated in equation 1.7.[60,61]

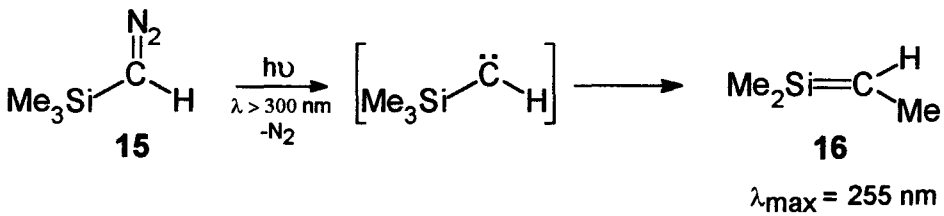

1.7

Therefore, by using a low temperature matrix, one can indefinitely stabilize the reactive intermediate[60-62] in question in order for direct characterization of the molecule by both infrared and ultraviolet spectroscopy.

1.3.3 Stabilized Silenes

The first *stable* silene was prepared and isolated by Brook and coworkers from the photolysis of acyldisilanes (**17**) as well as acylpolysilanes.[70-74] Photolysis of these compounds results in a [1,3]-Si shift to yield silene **18** (eq.1.8). The silenes can be observed in equilibrium with the corresponding dimer when the substituent is *tert*-butyl. Bulkier substituents (R') such as 1-adamantyl ($C_{10}H_{15}$), triethylmethyl (CEt3), 1-methyl-

cyclohexyl (C_7H_{13}) and mesityl (C_9H_{11}) stabilize the silene to allow isolation at room temperature, and characterization by ^{29}Si NMR.

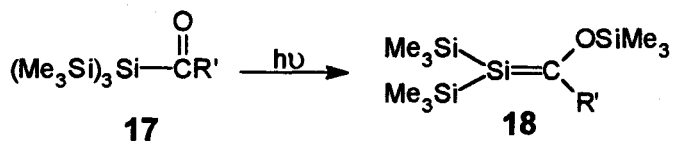

17 18 **1.8**

The X-ray crystal structure of **18** (R' = $C_{10}H_{15}$) reveals a Si=C bond length of 1.76 Å,[73] in good agreement with the theoretical predictions.[27,29,73,74]

1.3.4 Direct Detection of Transient Silenes in Solution

A number of reactive silenes have been generated, and detected[75,76,77-83] in solution using nanosecond laser flash photolysis techniques. To date, these studies have employed aryldisilanes or silacyclobutanes as photochemical precursors with detection of the silenes by transient UV absorption spectroscopy. This technique allows measurement of the UV absorption spectrum of a photochemically produced transient and measurement of its lifetime and rate constants for reaction with chemical trapping agents in solution.

The first finding of this type was published in 1985 by Ishikawa and coworkers who reported that the laser flash photolysis of pentamethylphenyldisilane (**11**) generated a reactive conjugated silene **12** as demonstrated in equation 1.9.[75]

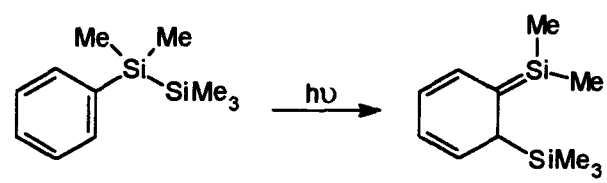

11 12 **1.9**

λ_{max} = 425 nm

Transient species **12** was found to have a UV absorption maximum centered at 425 nm[75] in cyclohexane at room temperature. The transient was reported to decay with single exponential decay kinetics and a lifetime of 4.8 μs.[75] It was reported that the lifetime (τ) of the 425 nm transient was very sensitive to the presence of moisture in the solvent used. The rate constant for reaction of **12** with ethanol (EtOH) in solution at room temperature was also measured.[75] The assignment and reactivity of this transient was later reinvestigated by Gaspar and coworkers[76] as well as by Leigh and Sluggett.[77-83]

Another report of this type was documented in a 1992 Bachelor of Science thesis[84] where nanosecond laser flash photolysis of **6** with 248-nm light in both acetonitrile and isooctane solution was found to generate a transient species which absorbed at 325 nm[84] in solution at room temperature as illustrated in equation 1.10.[84]

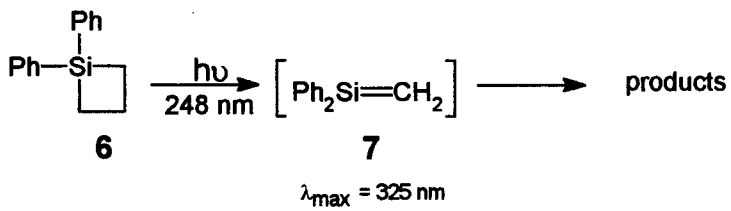

1.10

On the basis of the observed absorption maximum and steady-state photolysis product studies, the transient was assigned as 1,1-diphenylsilene (**7**).[84] The flash photolysis result was the first direct observation of this reactive organosilicon compound in solution at room temperature. Rate constants (k_q) for quenching of **7** by acetone and methanol were measured using *NLFP* techniques. Quenching of **6** in isooctane by acetone was found to be linear in concentration with a bimolecular quenching rate constant (k_q) of $(8.8 \pm 0.3) \times 10^7 M^{-1}s^{-1}$.[84,85] Quenching of **7** by methanol was quite rapid ($k \geq 10^8 M^{-1}s^{-1}$), but generated a nonlinear quenching plot. A deuterium kinetic isotope effect (KIE) k_H/k_D

of 1.3[84,85] was measured by steady-state product analysis for the reaction of **7** with methanol.

It was reported by Leigh and coworkers that nanosecond laser flash photolysis of 1,1,2-triphenylsilacyclobutane (**19**)[86] gave rise to a transient species centered around 323 nm,[86] which was assigned to **7** based on comparison with the carbon analogue as well as comparison with previous data for 1,1-diphenylsilacyclobutane.[86]

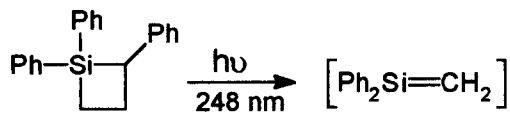

19 **7** **1.11**

The silene **7** was found to decay on the microsecond timescale with mixed first- and second-order kinetics in deoxygenated isooctane solution. The lifetime (τ) of **7** was found to be 13 μs.[86] Compared with the silatriene intermediate (**12**), **7** was found to be relatively unreactive toward oxygen where the quenching rate constant was experimentally determined to be $k_q \approx 5 \times 10^6 M^{-1}s^{-1}$.[86] Other trapping agents such as alkanones, ethyl acetate, and 2,3-dimethyl-1,3-butadiene were used to quench the silene. Quenching with alcohols was not studied due to the fact that **19** undergoes a dark reaction with alcohols to give the acyclic silyl methyl ether **20** shown in equation 1.12.[86]

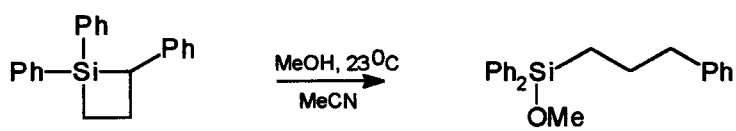

19 **20** **1.12**

1.4 Previous Studies Regarding Alcohol Addition to Silenes

The mechanism of alcohol addition to silenes has been a subject of much controversy since the early 1980's.[16,26,74,77,87,88] This section will review the basic features of the addition of alcohols to silenes; *i.e.*, the stereochemistry,[74,87,88] the relative rates,[16] the mechanisms,[16,26] and ab initio calculations[96,97] for alcohol addition to silenes. Finally, absolute rate constant measurements using nanosecond laser flash photolysis will be introduced.[73,74,77-86]

1.4.1 Stereochemistry of Alcohol Addition

The addition of methanol to silenes was observed to occur with high *syn-stereoselectivity* by Jones and coworkers.[87] It was found that a mixture of the anthracene adducts **21a** and **21b** could be isolated from the addition of anthracene to [α-(trimethylsilyl)vinyl]methylphenylchlorosilane with *t*-BuLi in benzene. The anthracene adducts were observed to undergo facile stereospecific decomposition at temperatures as low as 190°C to generate the corresponding silenes, **22a** and **22b**. Thermolysis of pure **21a** and **21b** in the presence of excess methanol led to the formation of the methanol adducts **23a** and **23b**, respectively as shown in Scheme 1.5. These results indicate that the reaction of methanol with silenes is stereospecific.

In 1985, Brook and coworkers investigated the effects of various substituents on the stability and chemistry of the stable solid silenes (**24a**).[73,74] It was found that upon

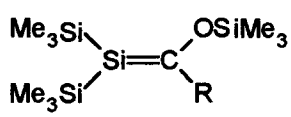

24a

R = 1-adamantyl

Scheme 1.5 Stereospecific Addition of Alcohols to a Silene

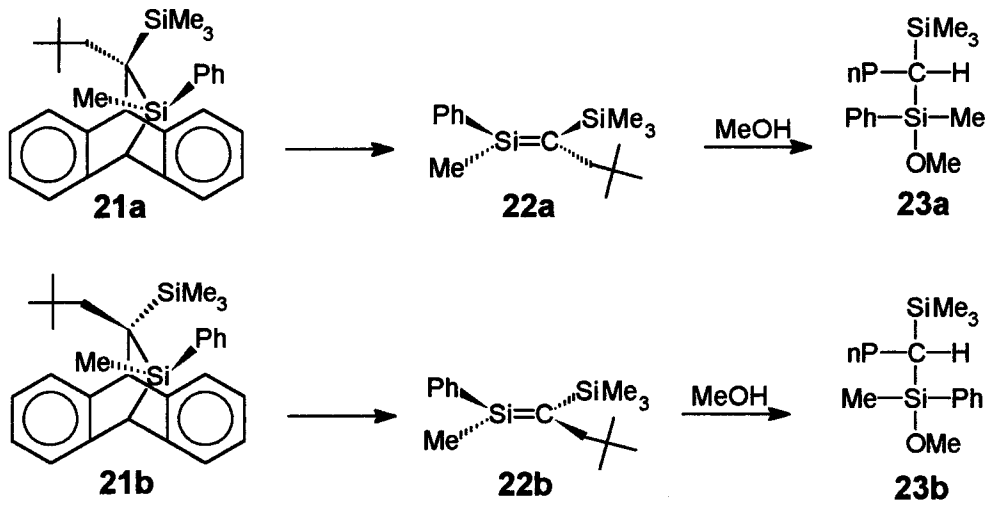

photolysis of the acylsilane (**24a**) in the presence of methanol two diastereomeric products of the corresponding silene were generated (eq.1.13).[74]

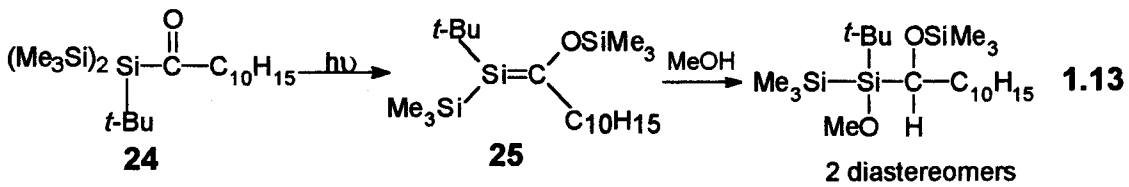

A few years later in 1991, Sakurai and coworkers[88] published results pertaining to the stereochemistry and mechanism of alcohol addition to a transient cyclic vinylsilene **28** generated by the photolysis of disilane **27** as shown in equation 1.15.[88] It was reported this reaction yields two stereoisomeric products, **29a** and **29b**, and that the relative yields of the two vary with the concentration and acidity of the alcohols.[89,90]

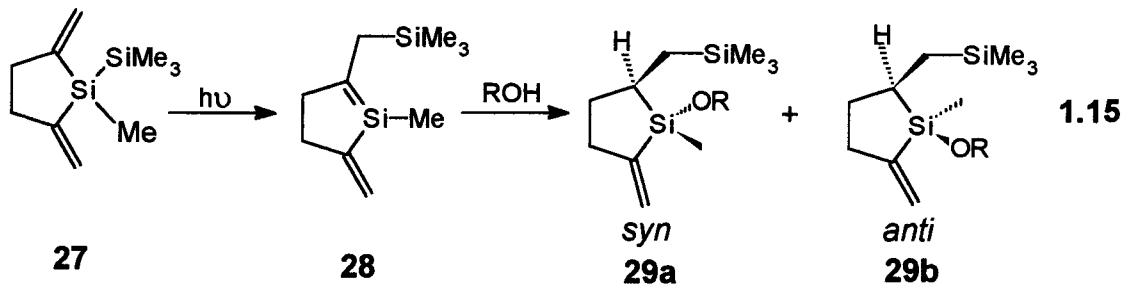

The *syn/anti* product ratio, **29a/29b**, was found to increase in the following order: methanol < 2-propanol < < *tert*-butyl alcohol, where *tert*-butyl alcohol gave only the *syn* product.[88]

1.4.2 Mechanism of Alcohol Addition

In 1984 Wiberg[16] investigated the reaction of 1,1-dimethyl-2,2-bis(trimethylsilyl)-silene (**31**), generated by the thermal [2+2]-cycloreversion of **30**, with a series of alcohols. It was reported that the relative rates of reaction of **31** to alcohols depended on the nucleophilicity and steric bulk of the alcohol (eq.1.16).

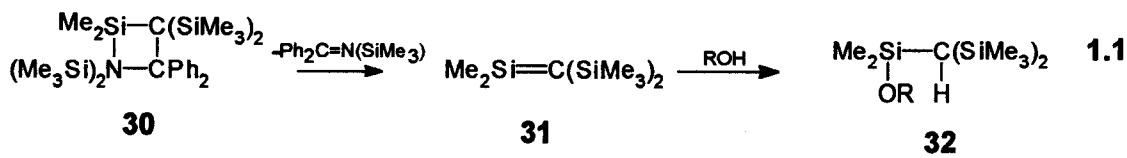

The relative rates of alcohol addition to **31** at 100°C in ether were found to follow the order: methanol > ethanol > 2-propanol > *tert*-butyl alcohol > 1-pentanol > cyclohexanol > phenol.[16] These results suggest that since the most acidic alcohol reacts the slowest, the first step of the reaction is addition of the nucleophile. In contrast, in electrophilic additions of alcohols to alkenes, the proton of a strong acid first adds to the double bond to yield a carbocation which is then attacked by the corresponding nucleophile (eq.1.17).[91]

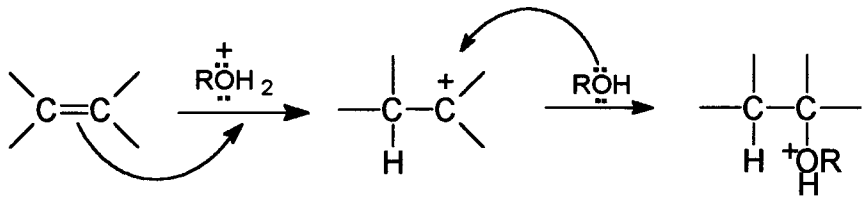

1.17

The nucleophilic mechanism was justified by the relative rates of addition of methanol, and methanol-d and the fact that acetic acid reacted more slowly than methanol.[16] The relative rates obtained from this study indicated that the mechanism of alcohol addition involves initial nucleophilic attack by the oxygen atom of the alcohol molecule onto the silicon atom of the silene **31** to form a Lewis acid-base complex. This complex then collapses to product (**32**) by fast proton-transfer to the carbon atom (eq 1.18).[16]

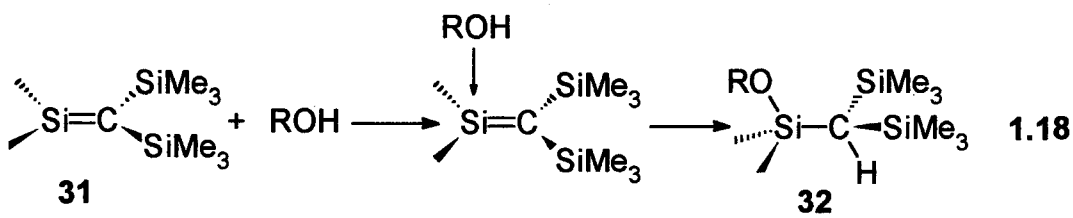

31 **32** 1.18

Sakurai and coworkers published results pertaining to the stereochemistry of alcohol addition to a cyclic divinylsilene **28** (Section 1.4.1, page 16).[88] Photolysis of the cyclic divinyldisilane **27** generated the cyclic silene **28** which was trapped by various alcohols to yield a mixture of *syn* **29a** and *anti* **29b** alcohol adducts (eq.1.15).[88] A linear correlation was found by plotting the *syn/anti* ratio versus the inverse of the alcohol concentration for each alcohol studied according to equation 1.19.[88] The slope of this line yields the rate ratio for formation of the two products formed, k_{syn}/k_{anti}. This rate ratio describes the relative reactivity of the complex towards *intra-* versus *inter*molecular proton transfer.

$$\frac{d[syn]}{d[anti]} = \left(\frac{k_{syn}}{k_{anti}} \right) \times \frac{1}{[ROH]} \qquad \textbf{1.19}$$

The rate ratio k_{syn}/k_{anti} for the addition of methanol, 2-propanol, and *tert*-butyl alcohol was found to be 5, 32, and ∞, respectively.[88] Based on these results a more detailed mechanism for the addition of an alcohol to a cyclic silene was proposed as shown in Scheme 1.6.[88] The mechanism proceeds with initial nucleophilic attack at the silicon atom by the oxygen from the alcohol to yield a silene-alcohol complex[86] as previously proposed by Wiberg.[16] Sakurai proposed that the silene-alcohol complex proceeds to product by either *intra*molecular proton transfer (k_{syn}) leading to product **29a**, or *inter*molecular proton transfer (k_{anti}) from a second molecule of alcohol to yield adduct **29b**.[88] This proposed mechanism was justified based on a correlation of product distributions with the pK_a's of the alcohols.[88] That is, the pK_a of the protonated alcohol was used to model the pK_a of the silene-alcohol complex. This model was used as a measure of the propensity of the proton (H^+) to migrate to the carbon. The rate of *intra*molecular (k_{syn}), and *inter*molecular (k_{anti}) proton transfer was found to be directly proportional to the pK_a of the protonated alcohols (ROH_2^+) and the unprotonated alcohols (ROH), respectively.[88]

Scheme 1.6 Alcohol Addition to a Cyclic Silene

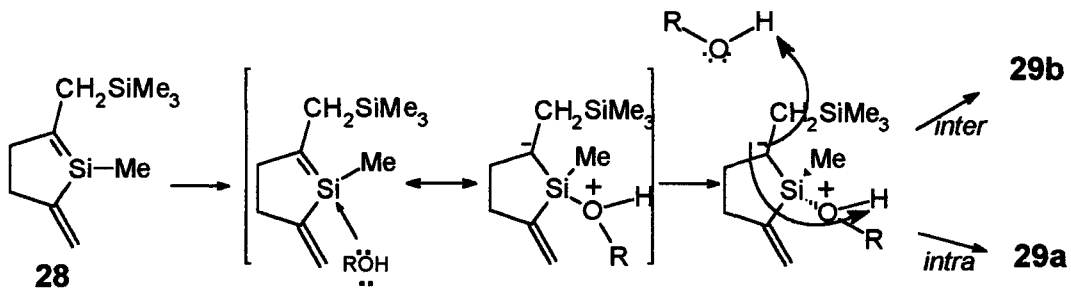

1.4.3 Direct Rate Constant Measurements for Silene Trapping Reactions

The most general approach to reaction mechanism elucidation is through both kinetic and product studies.[92] *NLFP*[93,94] is a transient spectrosopic technique that can be used to characterize reactive intermediates in solution at room temperature. This technique was one of the tools used to propose a mechanism for the addition of alcohols to a simple silene.

Figure 1.3 shows a simple schematic of the nanosecond laser flash photolysis apparatus.[93] Essentially, the *NLFP* system is a UV spectrometer capable of very fast response to changes in sample absorbance. An excimer laser of a specific wavelength (248, 308 or 337 nm) is used to excite the sample and generate the reactive intermediate of interest. If this spectrometer is set at a monitoring wavelength in a region where the reactive intermediate absorbs, then a plot of solution optical density (O.D.) versus the time yields the decay profile of the intermediate.[93] An example is shown in Figure 1.4.[93] The rate of return of the absorbance to its pre-pulse value gives the rate of decay of the transient responsible for the absorption. A plot of the average transient optical density (O.D.) in a fixed time window after the laser pulse versus monitoring wavelength yields the UV spectrum of the transient, an example of which is shown in Figure 1.5.[84,85]

Addition of a reagent which reacts with the transient results in an increase in its decay rate and pseudo first order decay kinetics. A plot of transient decay rate versus quencher concentration according to equation 1.20 affords the bimolecular rate constant for reaction of the transient with the quencher, k_q.[93,94]

$$k_{decay} = k_o + k_q[Q] \qquad \textbf{1.20}$$

The following is an example of the direct rate constant measurement of a reactive intermediate. Leigh and Sluggett have studied the addition of classic silene traps with a transient conjugated silene.[77-83] The photolysis of an aryldisilane $PhMe_2SiSiMe_3$ generated the corresponding 1,3,5-(1-sila)hexatriene derivative (**12**) in equation 1.9 (page 12). Plots of k_{decay} versus [ROH] with non-acidic alcohols afford curved quenching plots which were quadratic in alcohol concentration.[77] Addition products were detected which were consistent with addition of water, methanol, ethanol, and *t*-butyl alcohol to the corresponding silatriene (**12**).[77] A small primary kinetic isotope effect of 1.7 was observed for water.[77] These results were interpreted in terms of a multistep mechanism involving rapid, reversible silatriene- alcohol complex formation, followed by competing rate-determining *intra*-or *inter*molecular proton transfer (Scheme 1.7).[77] This was the first clear demonstration of the involvement of proton transfer in the rate-determining step in the addition of alcohols to silicon-carbon double bonds. The proton transfer steps are rate-determining when the alcohol is only weakly acidic. More acidic and less nucleophilic alcohols such as 2,2,2-trifluoroethanol (TFE) and acetic acid (AcOH) follow strict second order kinetics in their reactions with silatrienes, and do not exhibit observable kinetic isotope effects (KIE).[77] This is consistent with rate-determining complex formation followed by rapid proton transfer. In order to verify the mechanistic

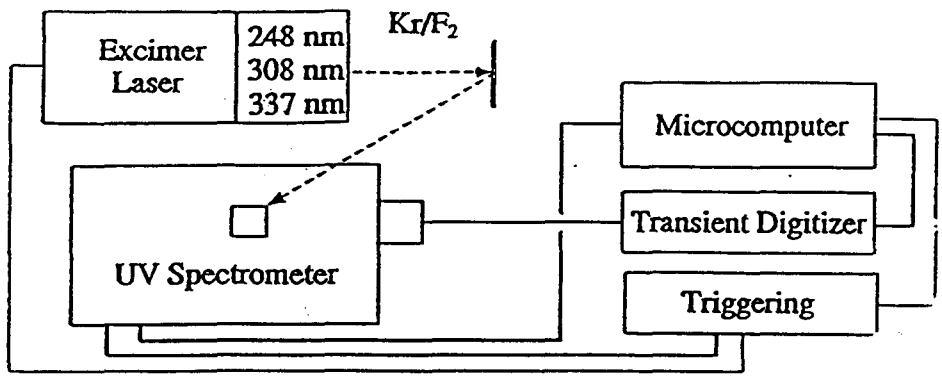

Figure 1.3 Schematic of the Nanosecond Laser Flash Photolysis Apparatus.

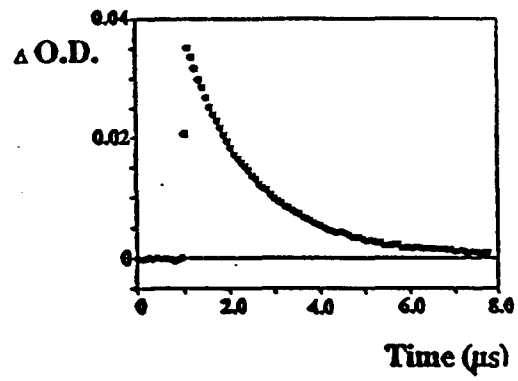

Figure 1.4 Transient Decay trace.

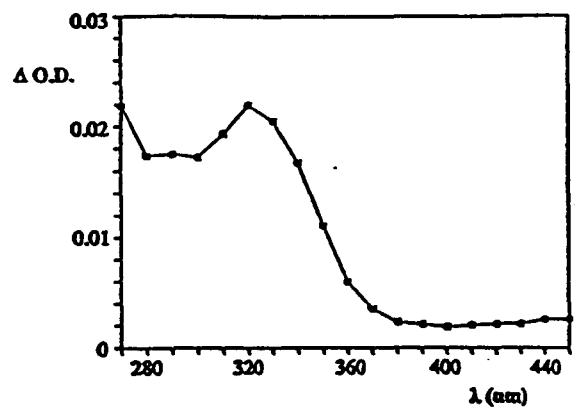

Figure 1.5 Transient Absorption Spectrum recorded 70-90ns after the laser pulse.

details of the reaction of alcohols with silatrienes, the addition of methanol was studied.[83] It was found that the quadratic dependence observed for methanol quenching is consistent with a mechanism involving fast, reversible formation of a silatriene-alcohol complex followed by competing *intra-* and *inter*molecular proton transfer.[83] A small primary KIE of 1.9 was observed for methanol[83] which verifies that proton transfer is rate-determining for the addition of non-acidic alcohols. The addition of more acidic compounds (TFE and AcOH) follows linear quenching kinetics, consistent with an inversion in the relative rates of complex formation and proton transfer. The lack of a KIE with AcOH(D) verifies that proton transfer is not involved in the rate-determining step. This supports proton transfer occurring after nucleophilic attack.[16,74,77,87,88] It was documented that the *inter*complex proton transfer reaction most likely occurs by a general base catalysis mechanism, involving deprotonation of the complex by alcohol, followed by rapid protonation.[83] Photolysis of pentamethylphenyldisilane (**11**) in acetonitrile containing 0.15 M methanol generated the following addition products: [1,2]-, [1,4]-, and [1,6]-addition of methanol to the silatriene.[83] Earlier work reported by Ishikawa[54] indicated that only the [1,4]- and [1,6]-addition products were isolated. It was found that the yield of the silatriene-alcohol products are dependent on the alcohol concentration for the addition of methanol to **12**.[83] At low alcohol concentrations (0.01 M), the [1,2]-addition product is the predominant product where the *intra*molecular proton transfer pathway is operative.[83] At high alcohol concentrations (0.1 M), the [1,4]- and [1,6]-addition products were observed.[83] At alcohol concentrations between 2-5 M, the yield of [1,4]-product increases with a decrease in the [1,2]- and [1,6]-addition products.[83] The variation in product distribution has been attributed to the involvement of alcohol oligomers in the product determining protonation step of the *inter*molecular proton transfer pathway.[83]

Scheme 1.7 Mechanism of Alcohol Addition to Silatriene (12)

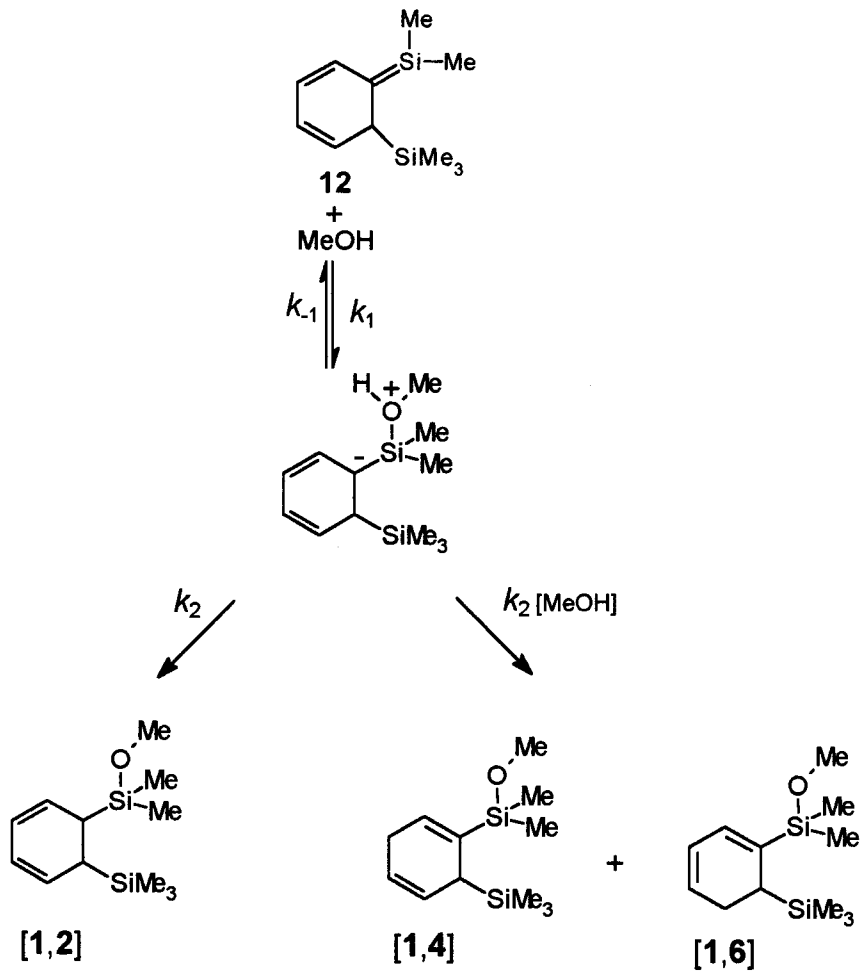

1.4.4 Ab initio Calculations Regarding the Mechanistic Addition of Polar Reagents to Silenes

Theoretical calculations[96,97] were performed in order to probe the addition mechanism of polar reagents with silenes. Two possible mechanistic pathways were investigated: electrophilic and nucleophilic addition. The study of electrophilic and nucleophilic addition was carried out using hydrochloric acid (HCl) and water (H_2O),

respectively. These types of addition reactions are exothermic in nature and proceed with initial formation of a weak complex in the early stage of the reaction. The transition state structures for the addition of HCl to both ethene and silaethene using the HF/6-31G* level were calculated.[96] The addition to ethene generated a four-centre transition state whereas addition to silaethene proceeded by a two-centre transition state. For the silaethene, it is important to note that Wiberg[16] proposed that for the addition of HCl (Lewis base), the chlorine attacks the electrophilic silicon atom of silaethene (Lewis acid) in a nucleophilic manner. The ab initio calculations illustrate that the carbon atom of the silaethene attacks the proton of HCl in an electrophilic fashion.[96,97] The transition state structures for the addition of water to both ethene and silaethene were calculated theoretically using the HF/6-31G* level.[97] Both transition state structures are similar to one another. The nucleophilic addition of water is evident in both structures. The lone pair of electrons on oxygen (H_2O) appears to interact with the π^* orbital of the ethene, and silaethene, respectively.

Therefore, the transition structures obtained using ab initio calculations at the HF/6-31G* level imply that HCl and H_2O add to silaethene in an electrophilic and nucleophilic manner, respectively.[96,97]

1.5 Objectives of this Work

To date, most of the evidence in favor of a silene intermediate has been based on indirect evidence from chemical trapping experiments.[9,11-18,20,22,23,44,45] What fascinated our research group was the fact that there were only a few recent studies[16,26,74,77,87,88] which have addressed the mechanism of alcohol addition. Both stereospecific[87] and non-stereospecific[74,88] addition of alcohols have been documented thereby raising the question as to whether the addition of alcohols to silenes is concerted or stepwise. Ab initio

calculations[96,97] have also been used to explain the mechanism of addition of polar reagents to silaethene. Therefore, it was of interest for our group to use transient spectroscopic techniques to generate and characterize reactive intermediates directly in solution at room temperature. It was initially proposed to study the reactivity of a simple silene using *NLFP*. The following precursors were studied: pentamethyl-phenyldisilane (**11**),[77-83] and 1,1,2-triphenylsilacyclobutane (**19**).[86]

The photolysis of pentamethylphenyldisilane **11**[77-83] (eq. 1.9, page 12) gave rise to a complex mixture of photoproducts thereby interfering with the direct characterization of the simple silene **7**. The characterization of the major photoproduct, the conjugated silene (**12**) generated from **11** was thoroughly studied,[77-83] and the dependence of k_{decay} on alcohol concentration was established. A stepwise mechanism was proposed based on the fact that the bimolecular quenching rate constant (k_q) was more sensitive to the nucleophilicity than acidity of the alcohols, and a primary kinetic isotope effect was observed for both water[77] and methanol.[83] The stepwise mechanism involved rapid initial formation of the silatriene-alcohol complex followed by competing, rate-determining, *intra*- and *inter*molecular proton transfer.[77-83] Since our research group now has substantial kinetic data to support the mechanism of alcohol addition to the conjugated silene, it is of much interest to monitor the reactivity of the simple silene directly.

A second precursor, 1,1,2-triphenylsilacyclobutane **19**[86] was analyzed (eq. 1.12, page 14) and was found to be susceptible to dark reactions in the presence of alcohols. Thus, it is not a good precursor for kinetic studies of the reaction of **7** with these reagents.

The approach to defining the mechanism of alcohol addition to simple silenes has only involved stereochemical[74,87-88] and chemical trapping experiments thus far. Sakurai proposed a mechanism based on product ratios for a cyclic silene **28** (eq. 1.15) as introduced in section 1.4.2 (page 17).[88] The only kinetic evidence for the mechanism of

alcohol addition to silenes was proposed by our group using silatriene **12**. Comparison of the kinetic data generated by Sakurai, and coworkers for **28**[88] to those obtained for **12**[77,83] suggests that the observable kinetic behavior of **7** might be very different from that of the silatriene **12**.

The ultimate goal of this work is to employ *NLFP* techniques[93,94] to detect and characterize the reactivity of **7** directly. The reactivity of the silene **7** will then be compared with the reactivity of the more highly conjugated silene **12**,[77-83] and the cyclic silene **28**[88] to further test the proposed mechanism for alcohol addition.

Therefore, this study will proceed by determining: the rate constants for addition of a variety of alcohols (of varying nucleophilicity, and acidity), the photoproducts generated in the presence of these alcohols and the kinetic isotope effects (KIE) for each alcohol to elucidate the mechanism for alcohol addition to **7**.

CHAPTER 2

RESULTS

2.1 Synthesis

1,1-Diphenylsilacyclobutane (**6**) was synthesized[98] from commercially available materials according to equation 2.1.

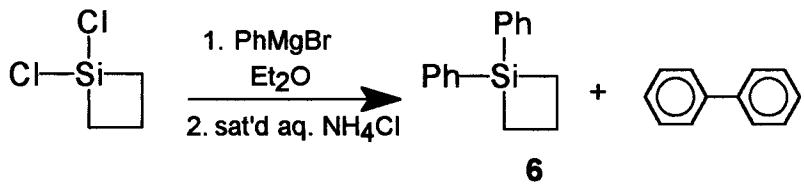

6 **2.1**

2.1.1 Purification of 1,1-diphenylsilacyclobutane 6

The purification of **6** was carried out by use of vacuum distillation. Two fractions were collected, and analyzed by gas chromatography (GC). The first fraction collected at 45°C (0.05 mmHg) was found to be that of the expected by-product, biphenyl, via GC coinjection of the distillate with an authentic sample.[99] The second fraction collected at 80°C (0.05 mm Hg) was found to contain two products. The major product was identified as **6** by GC/MS and ^{1}H-NMR spectroscopy. The ^{1}H NMR spectrum of the compound was consistent with previously published spectral data for **6**.[100] The ^{1}H-NMR spectrum of **6,** shown in Figure 2.1, shows a triplet centred around δ 1.5 ppm, a pentet located at δ 2.3 ppm, and a multiplet at δ 7.4-7.6 ppm. The second product accounted for approximately 10% of the sample and was identified as biphenyl. The silacyclobutane

was further purified by vacuum distillation, removing the majority of the biphenyl by repetitive vacuum sublimation. After four sublimations the product of interest, **6**, was distilled as a clear colourless oil, with a purity of 99.9% (0.1% biphenyl) by GC. The overall yield of **6** was 82%.

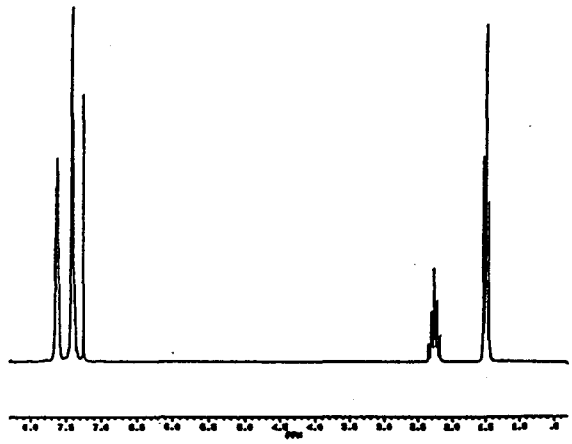

Figure 2.1 ^{1}H NMR (200 MHz) spectrum of purified 1,1-diphenylsilacyclobutane **6** recorded in $CDCl_3$.

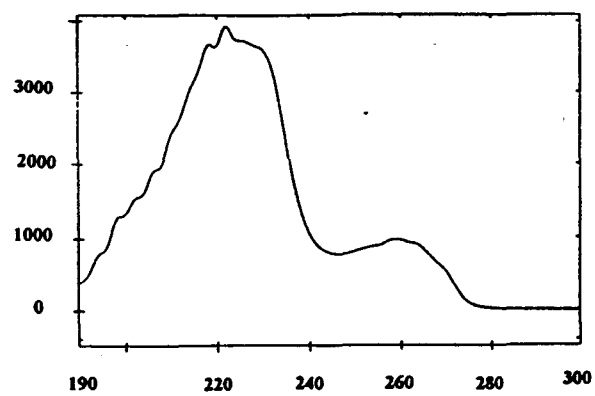

Figure 2.2 Ultraviolet absorption spectrum of a 6 x10^{-4} M solution of **6** in cyclohexane at room temperature (ε_{248} = 910 $M^{-1}cm^{-1}$).

2.2 Steady-State Ultraviolet Absorption Spectrum of 6

The static UV absorption spectrum of a 6 x 10^{-4} M solution of **6** in cyclohexane at room temperature is shown in Figure 2.2 (page 29) as a plot of molar extinction coefficient (ε) versus wavelength (nm). The spectrum shows the expected absorption maximum at 260 nm, corresponding to a benzenoid π,π* absorption.[101] The extinction coefficient (ε_{248}) was found to be 910 $M^{-1}cm^{-1}$.

2.3 Thermal Stability of 6 Towards Alcohols

The thermal stability of **6** in the presence of various alcohols was analyzed. Solutions of 0.1 M **6** in 1,1,1,3,3,3-hexafluoroisopropanol, 2,2,2-trifluoroethanol, and glacial acetic acid were allowed to stand at room temperature for *ca.* 72 hours. There was no observable decomposition of **6** (by GC or by GC/MS) over this period in any case.

2.4 Steady-State Photolysis of 6

The steady-state photolysis (254 nm) of **6** in isooctane in both the absence, and presence of various nucleophilic σ-bonded silene traps[16] has been carried out under similar conditions to those reported by Sommer and coworkers.[44] The following trapping agents were used: water (H_2O), methanol (MeOH), methanol-d (MeOD), ethanol (EtOH), ethanol-d (EtOD), *t*-butyl alcohol (*t*-BuOH), 2-propanol (*i*-PrOH), 2,2,2-trifluoroethanol (TFE), 1,1,1,3,3,3-hexafluoroisopropanol (HFIP), and acetic acid (AcOH).

In each steady-state photolysis whose progress was followed by GC, dodecane (0.005 M) was included in the solution as an internal GC standard.

A 0.01 M isooctane solution of **6** was photolysed in a Rayonet reactor using eleven 254 nm mercury lamps for three minutes in the absence of any trapping agents to *ca.* 10% conversion. GC analysis failed to reveal any detectable volatile product(s), although the

photolysate turned from a clear colourless solution to a translucent orange. The same result was observed in both polar (acetonitrile) and nonpolar (isooctane) solvents except for the fact that in acetonitrile, a photoproduct (**9**) consistent with the addition of water to **7** was detected by GC, and GC/MS as shown in equation 2.4.

Direct photolysis (254 nm) of a 0.01 M solution of **6** in isooctane containing 0.05 M MeOH to *ca.* 10% conversion afforded **8** as the only detectable photoproduct as shown in equation 2.2.

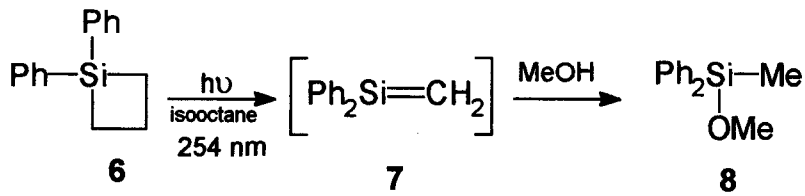

6 **7** **8** **2.2**

Product **8** was isolated by semi-preparative gas chromatography, and characterized by GC, GC/MS, ^{1}H-NMR, ^{13}C-NMR, FT-IR, mass spectrometry, and by coinjection of the photolysates with authentic samples prepared by the method shown in equation 2.3.[99]

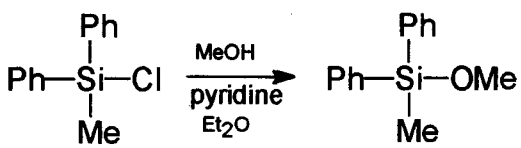

8 **2.3**

Authentic samples of the photolysates were also photochemically generated in the following manner. Isooctane solutions (10mL) of **6** 0.02 M in the presence of various alcohols (MeOH, EtOH, *i*-PrOH, *t*-BuOH, TFE, and HFIP; 0.01 M) were photolysed to conversions of approximately 65% (by GC analysis). The products **34**, **35**, **36**, **37**, **38**, and

39 were then isolated using semi-preparative gas chromatography followed by evaporation of solvent and excess alcohol. GC, GC/MS, ^{1}H-NMR, ^{13}C-NMR, FT-IR, and mass spectrometry were used to characterize the product.

Direct photolysis of a 0.01 M solution of **6** in acetonitrile (MeCN) containing 0.05 M methanol to *ca.* 10% conversion of **6** afforded **8** as the major photoproduct as well as small amounts of a product (**9**) consistent with the addition of water to **7** (eq. 2.4) which was detected by GC and GC/MS. The photolysis of a 0.01 M solution of **6** in the presence of water resulted in a single photoproduct which was identified as **9** by GC/MS as shown in equation 2.4.

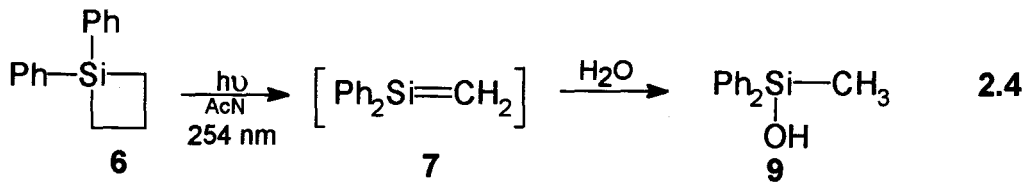

2.4

Steady-state photolysis of MeCN solutions (0.01 M) of **6** in the presence of EtOH, *t*-BuOH, *i*-PrOH, TFE, HFIP, and AcOH (0.05 M) under similar conditions afforded a single product in each case, consistent with alcohol addition to simple silene **7**. The products and their chemical yields (as percentage of consumed **6**) from the photolyses in MeCN solution are shown in Table 2.1.

Table 2.1 Summary of Primary Photoproducts generated from the addition of the corresponding alcohol, and their chemical yield after *ca.* 10% conversion of **6** in Acetonitrile (MeCN).[a]

Alcohol	Compound	Photoproduct	Chemical Yield (%)
MeOH	**34**	$Ph_2Si(OCH_3)CH_3$	70
EtOH	**35**	$Ph_2Si(OCH_2CH_3)CH_3$	65
***i*-PrOH**	**36**	$Ph_2Si(OCH(CH_3)_2)CH_3$	52
***t*-BuOH**	**37**	$Ph_2Si(OC(CH_3)_3)CH_3$	26
CF_3CH_2OH	**38**	$Ph_2Si(OCH_2CF_3)CH_3$	54
$(CF_3)_2CHOH$	**39**	$Ph_2Si(OCH(CF_3)_2)CH_3$	43
CH_3COOH	**40**	$Ph_2Si(OOCCH_3)CH_3$	61

a. The chemical yield was calculated relative to an internal standard, dodecane (0.005 M).

2.5 Nanosecond Laser Flash Photolysis

Nanosecond laser flash photolysis (*NLFP*)[93,94] experiments were carried out using a system which allows continuous flow of an oxygenated 3.1 x 10^{-3} M solution of **6** in dried acetonitrile. The flow system was required to replenish the contents of the sample cell.

A transient decay trace was measured using a fixed wavelength at which the transient of interest absorbs and monitoring the decay of the absorbance of the transient with respect to time. This was previously illustrated in Figure 1.4 (Section 1.4.3, page 22). A time-resolved UV absorption spectrum recorded 70-90 ns after flash photolysis of the oxygenated solution of **6** is illustrated in Figure 1.5 (Section 1.4.3; page 22). In isooctane solution, the transient exhibits a similar UV absorption spectrum to that in acetonitrile, but it is considerably longer lived (τ >5μs) and decays with mixed first- and second-order kinetics.

Original work consisted of identifying the transient species giving rise to the transient absorption spectrum generated upon flash photolysis of **6**. The transient decay trace (Figure 2.3(a)) shows residual absorption - clear evidence that there are two transients produced, a short-lived intermediate **7** shown in equation 2.2 as well as a longer-lived species. It was found that upon laser flash photolysis of a deoxygenated 3.1 x 10^{-3} M solution of **6** in acetonitrile, a broad absorption spectrum centered around 325 nm was observed as shown in Figure 2.3(b).[84] After extensive purification of **6** by several distillations (Section 2.1.1; page 28), the decay trace (Figure 2.4(a)) showed no evidence of residual absorption, thereby indicating that only one transient is produced with the purified sample. Figure 2.4(b) shows the corresponding transient absorption spectrum. Since biphenyl is formed as a side-product in the synthesis of **6**, it seemed likely that at least part of this additional complexity might have been due to biphenyl excitation.[102] Biphenyl triplets absorb strongly around 360 nm due to efficient intersystem crossing from

the first excited singlet state (S_1) to the triplet.[102] The lifetime (τ) of biphenyl triplet is known to exceed 10 μs in a deoxygenated solution.[102] Thus, the presence of minute quantities of biphenyl could lead to the formation of its triplet in addition to **7**. In order to test this hypothesis, a solution of 1.0×10^{-3} M authentic biphenyl was prepared, and a transient UV absorption spectrum in isooctane was recorded as shown in Figure 2.5. Upon comparison of Figure 2.4(b) and Figure 2.5, it is clear that the biphenyl triplet spectrum overlaps with that of the transient **7**. It was therefore proposed that Figure 2.3(b) contains biphenyl triplet as well as the shorter-lived transient **7**. It can clearly be seen by comparing the two transient absorption spectra, that the original sample of **6** was contaminated with biphenyl, as indicated by the formation of biphenyl triplets. The purity of **6** was found to be contaminated with approximately 1% biphenyl, as determined by gas chromatography.

Fractions containing less than 0.1% biphenyl were used for subsequent laser experiments, and solutions were oxygenated in order to reduce the lifetime of the biphenyl triplets substantially below that of **7**. Silene **7** is relatively unreactive toward oxygen ($k_q \approx 5 \times 10^6$ $M^{-1}s^{-1}$),[86] whereas biphenyl triplets are rapidly quenched by the presence of oxygen ($k_q > 10^9$ $M^{-1}s^{-1}$).[102] The transient absorption spectrum recorded is shown in Figure 2.6(b); it clearly shows the absorption due to **7** centered at 325 nm in acetonitrile (eq. 1.10; page 13).[84-86] The bimolecular quenching rate constants (k_q) for methanol, methanol-d, and 2,2,2-trifluoroethanol (Table 2.18; page 60) were studied in a nitrogen-saturated solution (using samples of **6** containing < 0.1% biphenyl) in order to verify whether the presence of oxygen has any effect on the rate of quenching of **7** by alcohols. Another laser experiment to further test the effects of oxygen on the quenching rate constant employed *trans*-piperylene to selectively quench biphenyl triplets.[102] The rate

constant for quenching of **7** by methanol in a nitrogen saturated 1.0×10^{-3}M acetonitrile solution of **6** containing 1.0×10^{-3} M *trans*-piperylene was found to be $(1.36 \pm 0.17) \times 10^{9}$ $M^{-1}s^{-1}$, in satisfactory agreement with the value obtained in oxygen saturated acetonitrile ($(1.40 \pm 0.04) \times 10^{9}$ $M^{-1}s^{-1}$). The bimolecular quenching rate constant (k_q) of **7** by *trans*-piperylene in isooctane was found to be $(8.07 \pm 0.45) \times 10^{6}$ $M^{-1}s^{-1}$.

The time-resolved UV absorption spectra of **7** in acetonitrile, isooctane, and hexane are shown in Figures 2.6(b), 2.7(b), and 2.8(b), respectively, along with the corresponding transient decay traces. It is evident that a maximum occurs at 325 nm in each solvent. Similar spectra, assigned to transient **7**, have been reported for *NLFP* of 1,1,2-triphenyl-silacyclobutane[86] in both deoxygenated acetonitrile and isooctane solution.

The transient UV absorption spectrum of **7** in THF is broadened, and shifted to longer wavelengths, with a maximum centered around 365 nm as shown in Figure 2.9(b). This is consistent with complexation of the silene with this solvent, as reported previously for other silenes.[79] There is no detectable difference in transient lifetime in nitrogen- and oxygen-saturated THF solutions.

The initial lifetime (τ_o) of **7** is strongly dependent on the presence of water in the sample, ranging from 308 ns in acetonitrile distilled from CaH_2[103] to a maximum of 4 μs in acetonitrile dried by passage through activated neutral alumina.[103] The concentration levels of water can be determined by using the bimolecular quenching rate contants (k_q) determined for water (Table 2.4) in equation 1.20[93,94] (Section 1.4.3; page 21). The concentration levels of water were estimated to be 0.8 mM and 0.3 mM, respectively.

The addition of alcohols or acetic acid to isooctane or acetonitrile solutions of **6** results in a reduction in transient lifetime. In both solvents, the transient decays with clean pseudo first-order kinetics in the presence of quenchers, and the lifetime is inversely

proportional to quencher concentration. Bimolecular quenching rate constants (k_q) were determined by linear least squares analysis of lifetime-concentration data according to equation 1.20[93,94] (Section 1.4.3, page 21).

Typical quenching plots for water, and a series of alcohols are shown in Figures 2.10 through 2.17. Tables 2.2-2.3 list bimolecular quenching rate constants (k_q) for quenching of **7** by various alcohols in hexane, and tetrahydrofuran solution. Tables 2.4-2.16 (pages 51-58) summarize the bimolecular quenching rate constants (k_q) for quenching of **7** by these compounds in dried oxygenated acetonitrile solution. *Average* bimolecular quenching rate constants (k_q) at 21 ± 1 °C, 25 ± 1 °C, and 28 ± 1 °C are listed in Table 2.17. The temperature at which the data was collected as well as the errors present in the lifetime (τ_o), and bimolecular quenching rate constant (k_q) are given at the end of Table 2.3. The method used to calculate the errors as also used for the remaining tables listed thereafter unless otherwise stated.

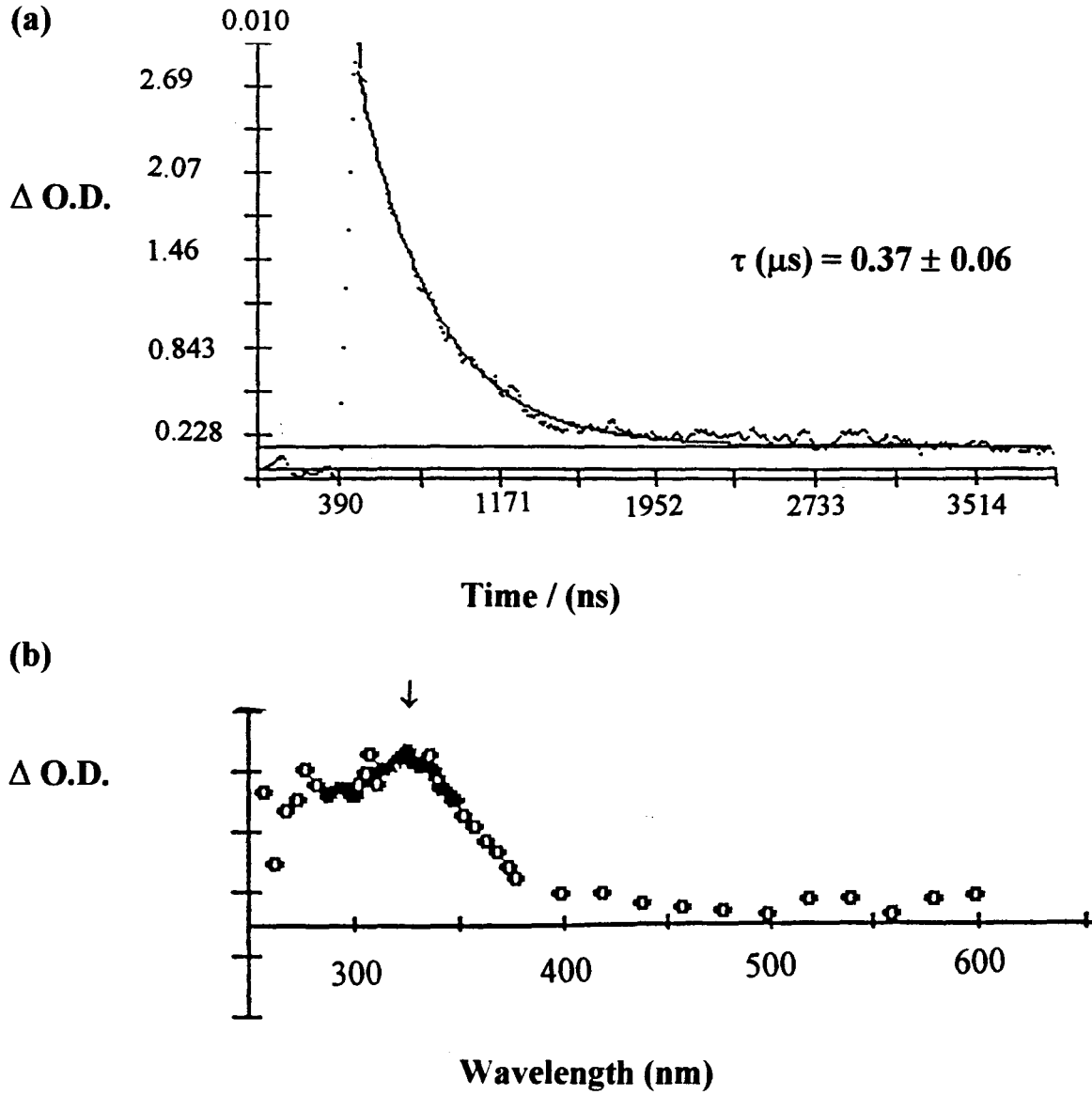

Figure 2.3 **(a)** ***Transient Decay Trace***: Recorded at 325 nm from 248 nm nanosecond laser flash photolysis of an oxygenated 3.1 x 10^{-3} M solution of **6** at 22 °C.
(b) ***Transient Absorption Spectrum***: Recorded 117-332 ns after 248 nm nanosecond laser flash photolysis of a deoxygenated 3.1 x 10^{-3} M solution of **6** in dry acetonitrile at 22 °C.

(a)

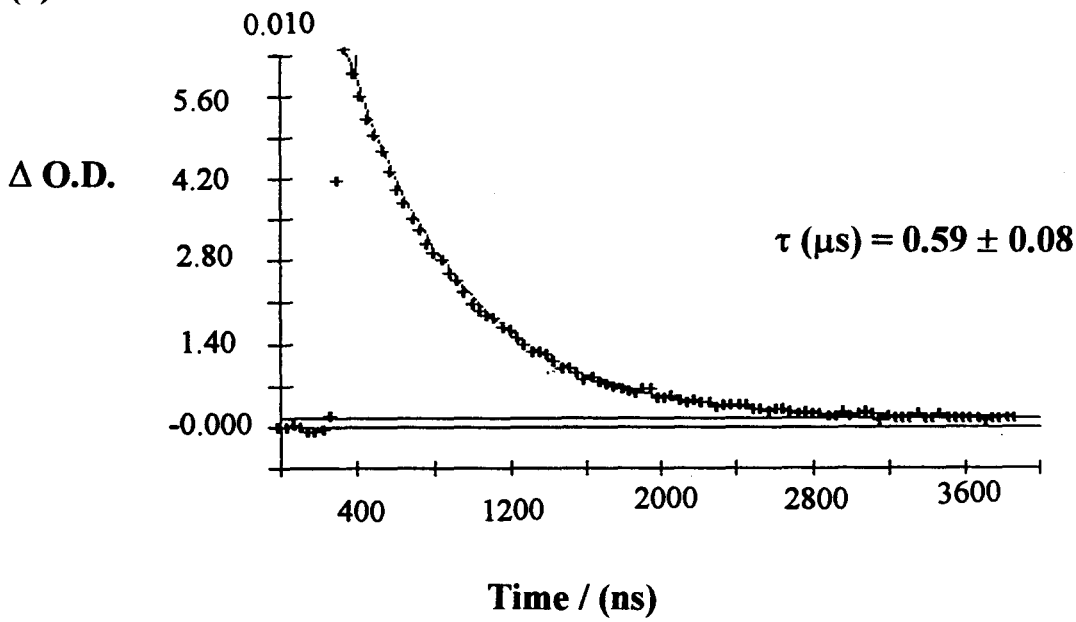

(b)

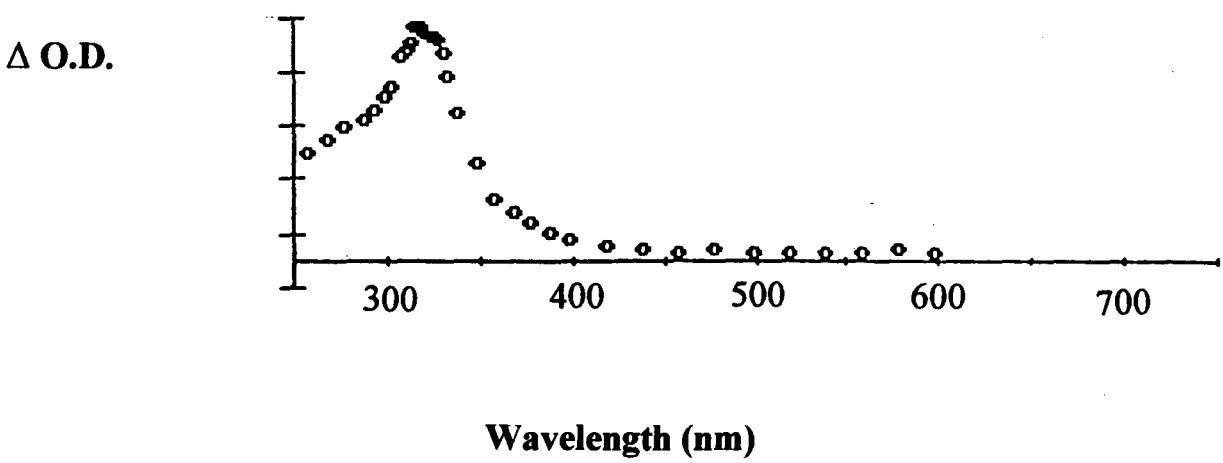

Figure 2.4 **(a)** ***Transient Decay Trace***: Recorded at 325 nm from 248 nm nanosecond laser flash photolysis of an oxygenated 3.1 x 10^{-3} M solution of **6** at 22 °C.
(b) ***Transient Absorption Spectrum***: Recorded 391-861 ns after 248 nm nanosecond laser flash photolysis of an air-saturated 3.1 x 10^{-3} M solution of **6** in acetonitrile at 21.9 °C.

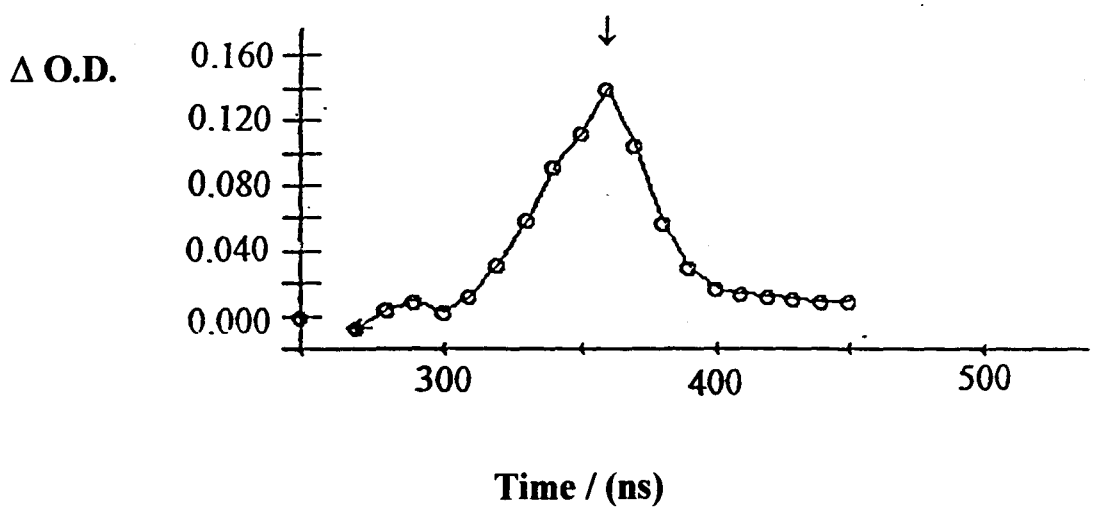

Figure 2.5 **(a)** ***Transient Absorption Spectrum***: Recorded following laser excitation from NLFP of a deoxygenated 3.0 x 10^{-3} M solution of biphenyl in isooctane at 23.2 °C.

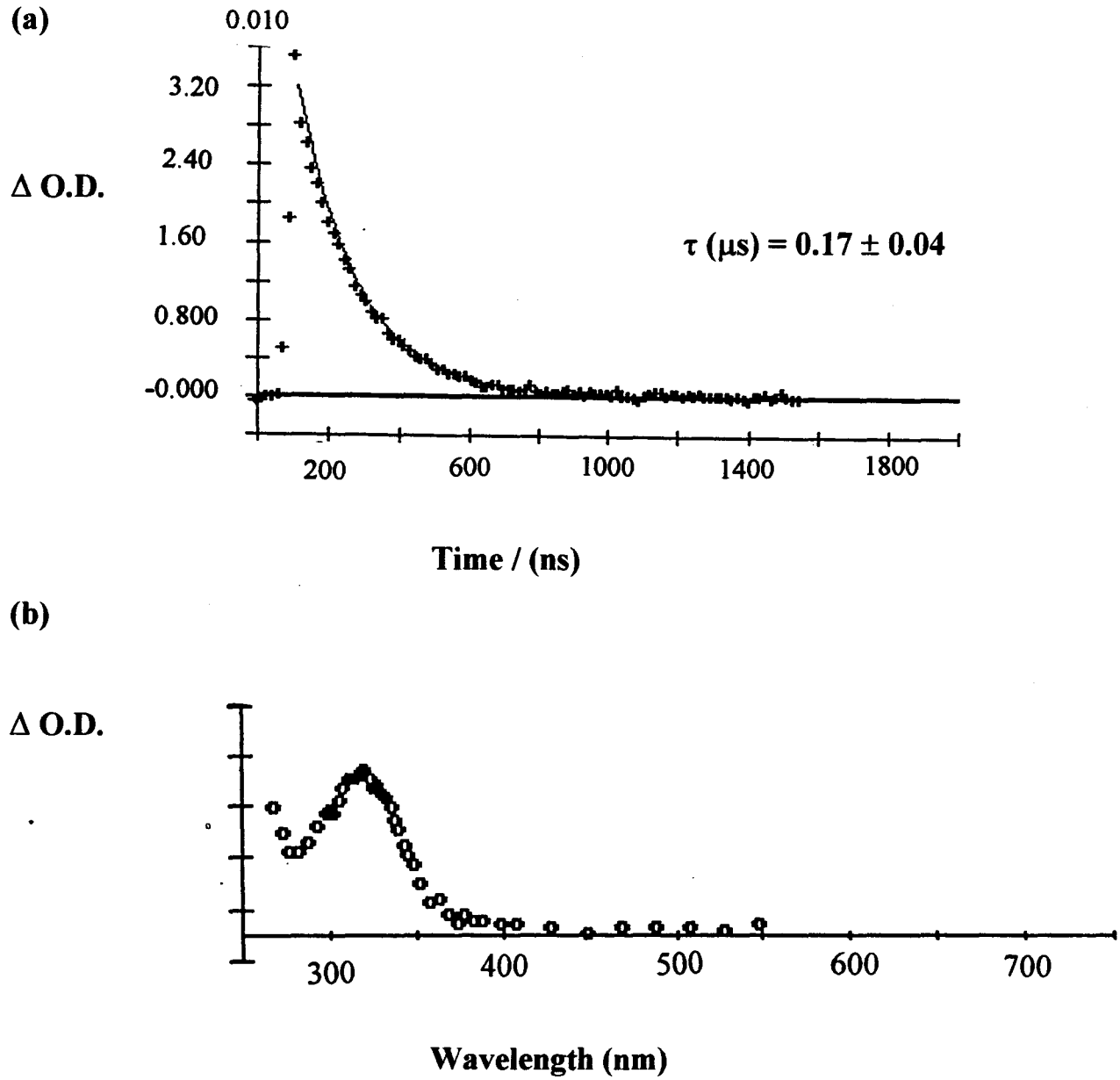

Figure 2.6 **(a)** ***Transient Decay Trace***: Recorded at 325 nm from 248 nm nanosecond laser flash photolysis of an oxygenated 3.1 x 10^{-3} M solution of **6** in acetonitrile at 22.8 °C.
(b) ***Time-resolved UV Absorption Spectrum***: Recorded 125-485 ns after 248 nm nanosecond laser flash photolysis of an oxygen-saturated 3.1 x 10^{-3} M solution of **6** in acetonitrile (MeCN) at 22.8 °C.

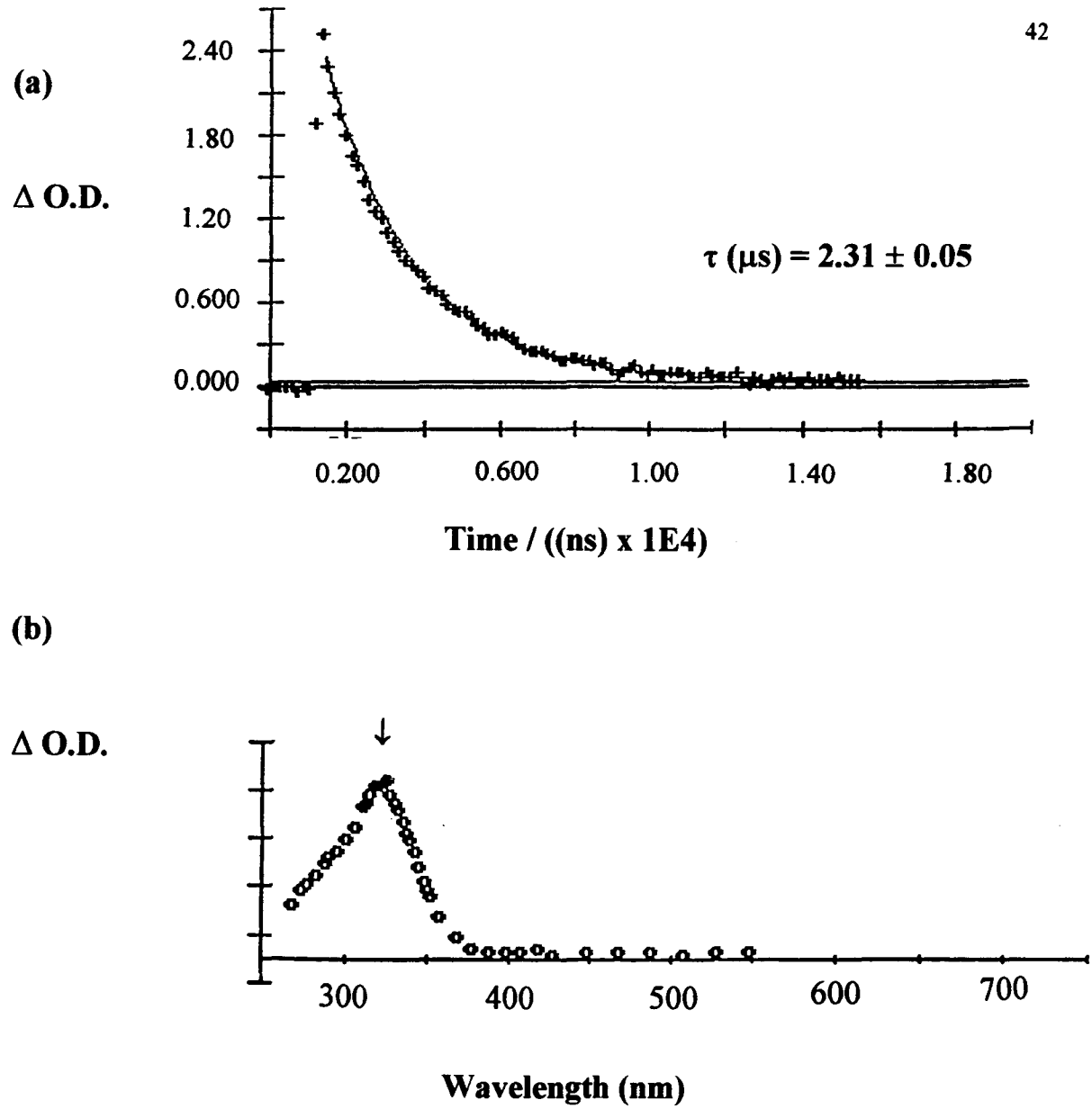

Figure 2.7 **(a)** ***Transient Decay Trace***: Recorded at 325 nm from 248 nm nanosecond laser flash photolysis of an oxygenated 3.1 x 10^{-3} M solution of **6** in Isooctane at 21.7 °C.
(b) ***Time-resolved UV Absorption Spectrum:*** Recorded 1.6-4.7 μs after 248 nm nanosecond laser flash photolysis of an oxygen-saturated 3.1 x 10^{-3} M solution of **6** in Isooctane at 21.7 °C.

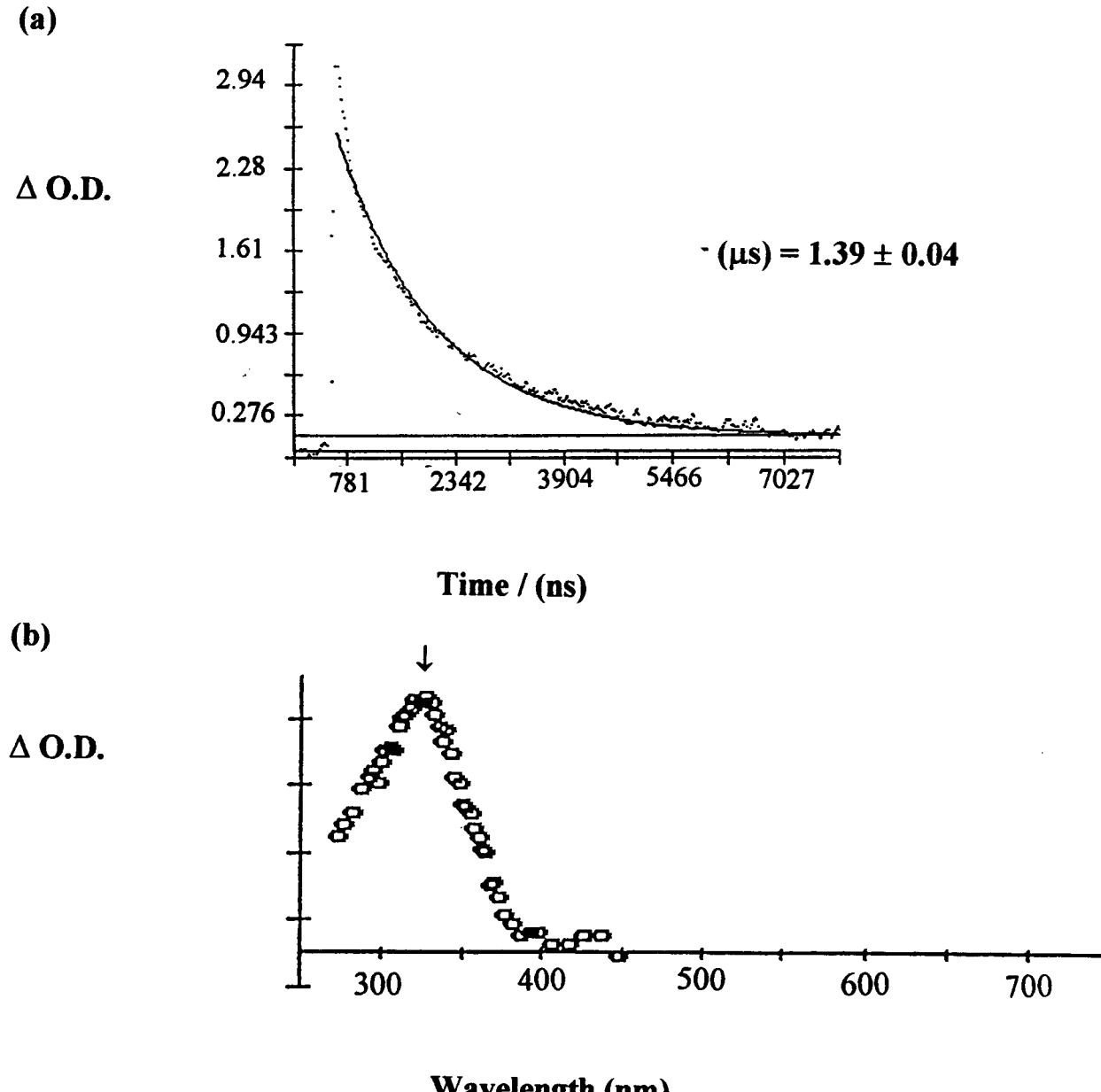

Figure 2.8 **(a)** ***Transient Decay Trace***: Recorded at 325 nm from 248 nm nanosecond laser flash photolysis of an oxygenated 3.1 x 10^{-3} M solution of **6** in Hexane at 22.4 °C.
(b) ***Time-resolved UV Absorption Spectrum***: Recorded 176-509 ns after 248 nm nanosecond laser flash photolysis of an oxygen-saturated 3.1 x 10^{-3} M solution of **6** in Hexane at 22.4 °C.

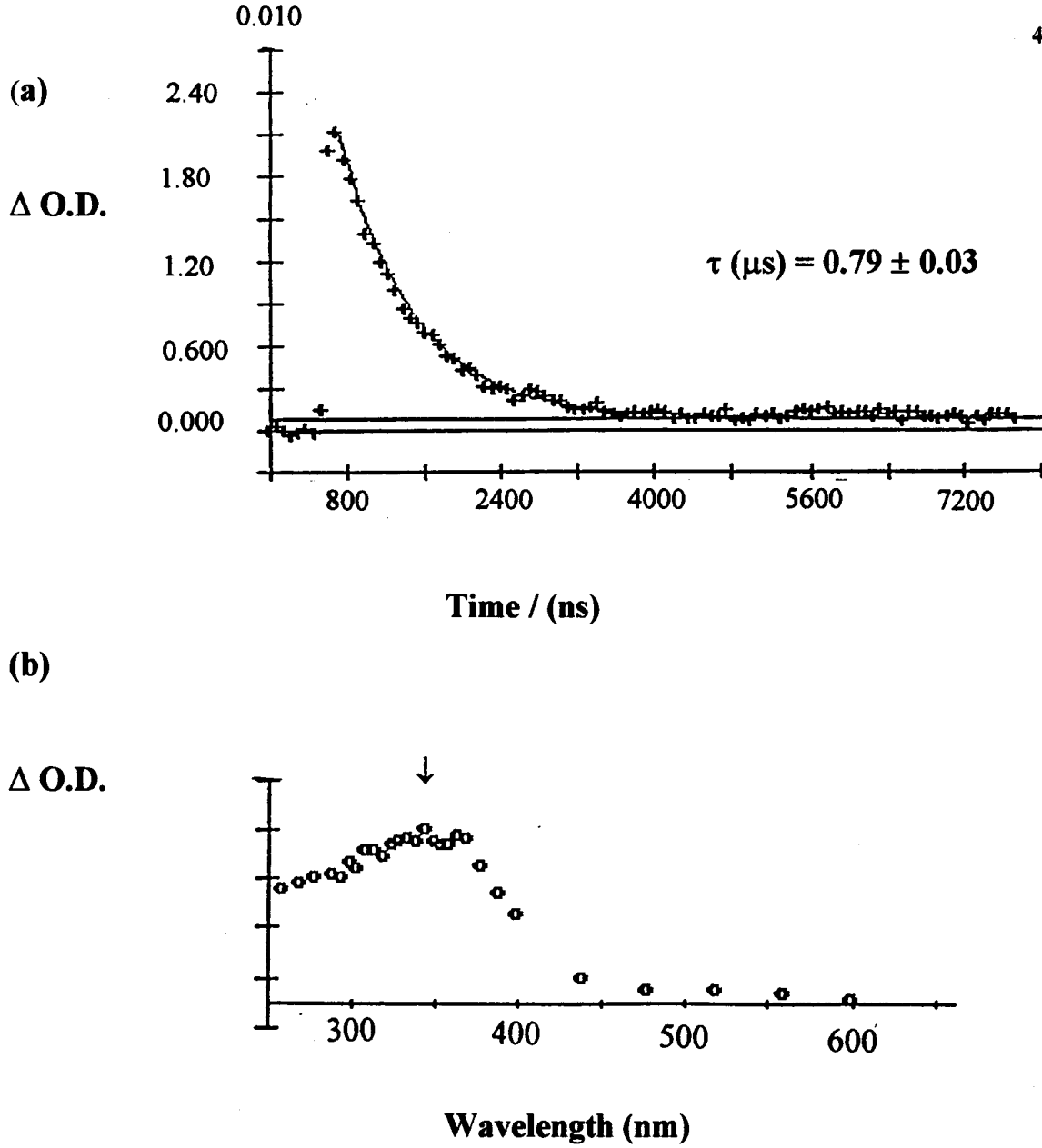

Figure 2.9 **(a)** ***Transient Decay Trace:*** Recorded at 325 nm from 248 nm nanosecond laser flash photolysis of an oxygenated 3.1 x 10^{-3} M solution of **6** in Tetrahydrofuran at 21.6 °C.
(b) ***Time-resolved UV Absorption Spectrum***: Recorded 0.8-1.4 μs after 248 nm nanosecond laser flash photolysis of an oxygen-saturated 3.1 x 10^{-3} M solution of **6** in Tetrahydrofuran at 21.6 °C.

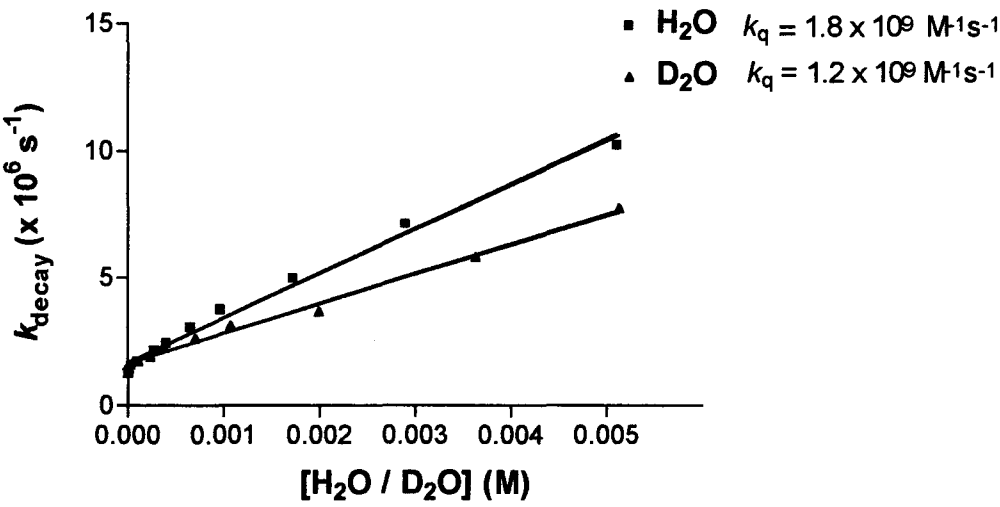

Figure 2.10 Quenching plots of k_{decay} of 7 versus quencher concentration for: Water (■) (20.7 °C) and Deuterium oxide (▲) (21.1 °C) in MeCN (Table2.4).

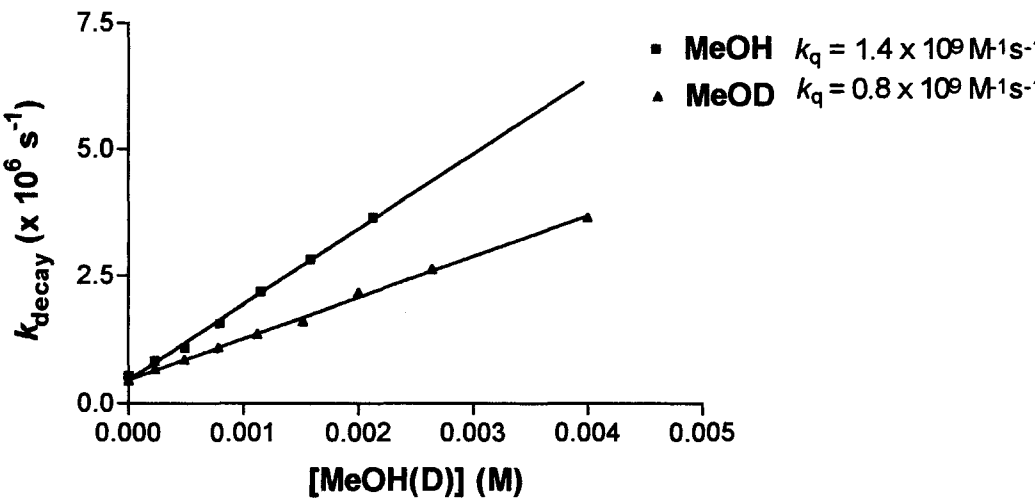

Figure 2.11 Quenching plots of k_{decay} of 7 versus quencher concentration for: Methanol (■) (28.9 °C) and Methanol-d (▲) (28.0 °C) in MeCN (Tables 2.5-2.6).

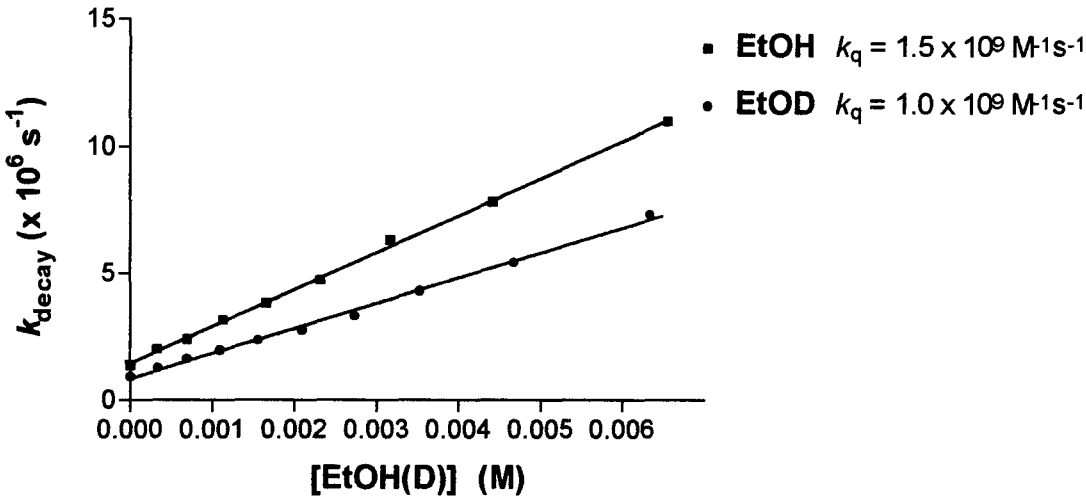

Figure 2.12 Quenching plots of k_{decay} of **7** versus quencher concentration for: Ethanol (■) (25.0 °C) and Ethanol-d (▲) (21.0 °C) in MeCN (Tables 2.7-2.8).

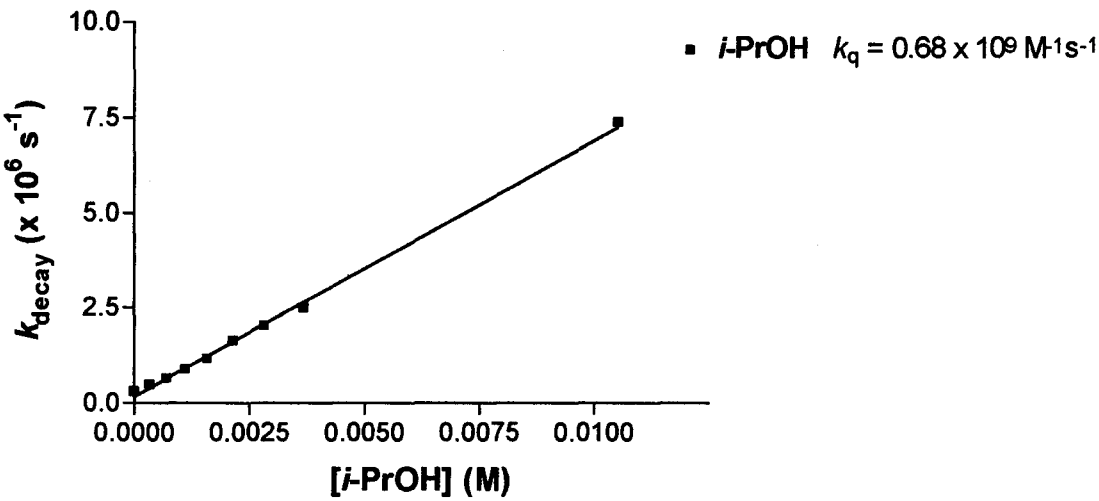

Figure 2.13 Quenching plot of k_{decay} of **7** versus quencher concentration for 2-Propanol (■) in MeCN at 24.7 °C as shown in Table 2.9.

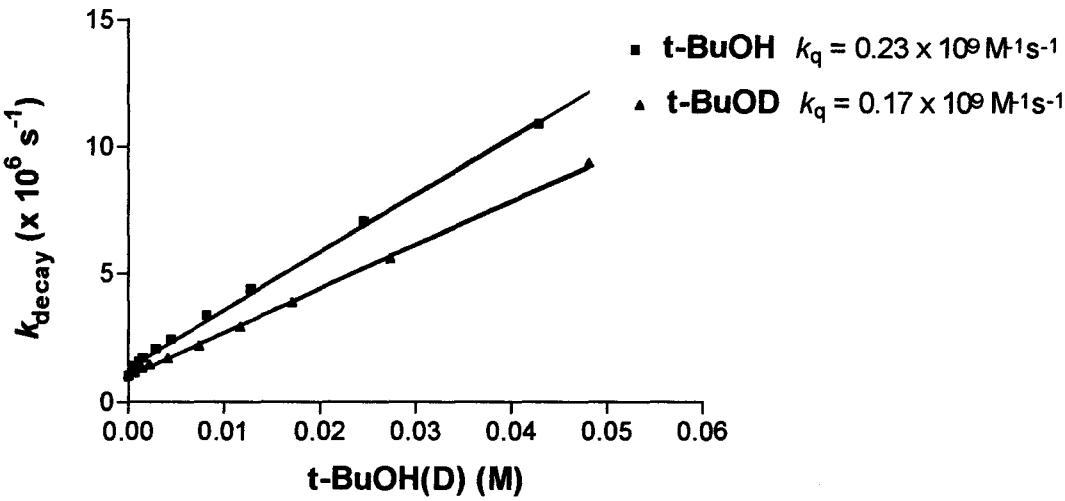

Figure 2.14 Quenching plots of k_{decay} of 7 versus quencher concentration for: *t*-butyl Alcohol (■) (23.0 °C) and *t*-butyl Alcohol-d (▲) (24.2 °C) in MeCN (Tables 2.10-2.11).

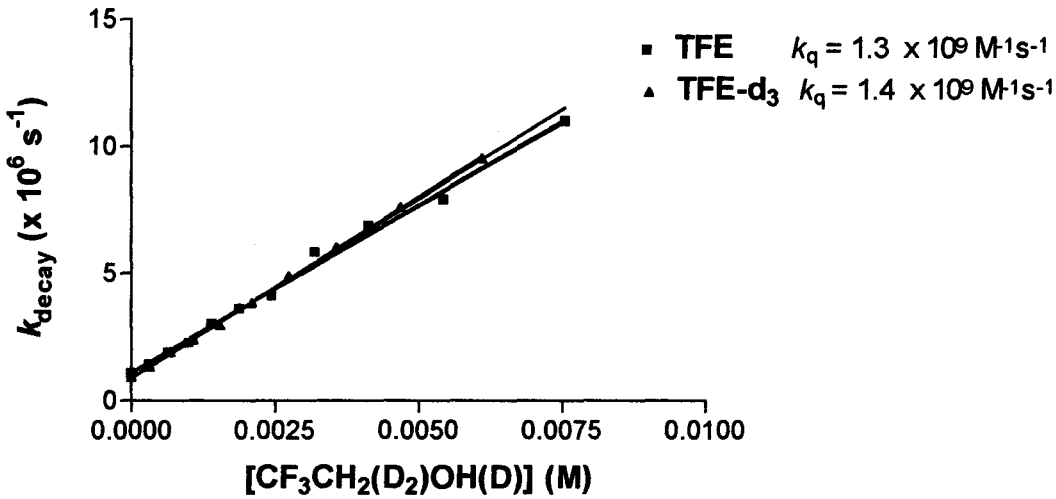

Figure 2.15 Quenching plots of k_{decay} of 7 versus quencher concentration for: 2,2,2-trifluoroethanol (■) (20.8 °C) and 2,2,2-trifluoroethanol-d_3 (▲) (21.0 °C) in MeCN (Tables 2.12-2.13).

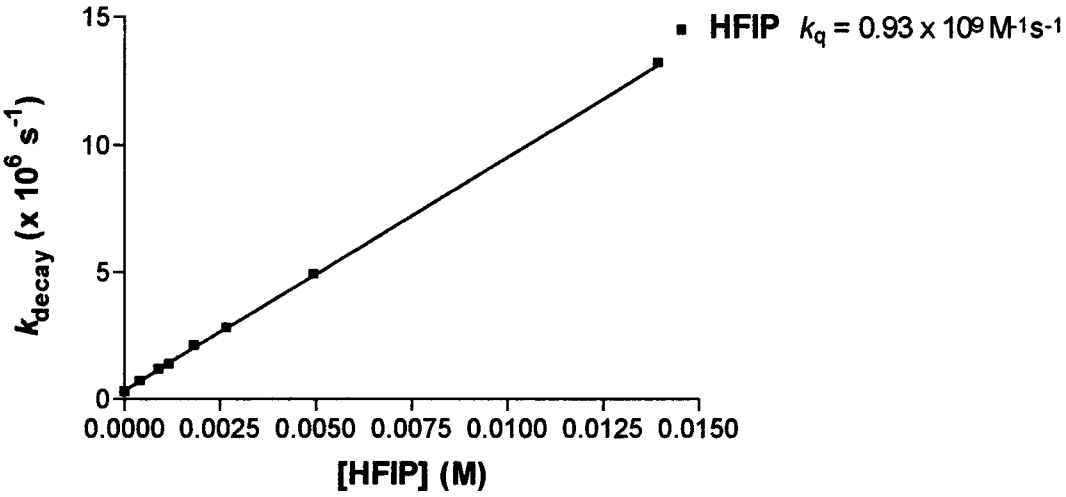

Figure 2.16 Quenching plot of k_{decay} of 7 versus quencher concentration for 1,1,1,3,3,3-Hexafluoroisopropanol (■) in MeCN at 24.6 °C as shown in Table 2.14.

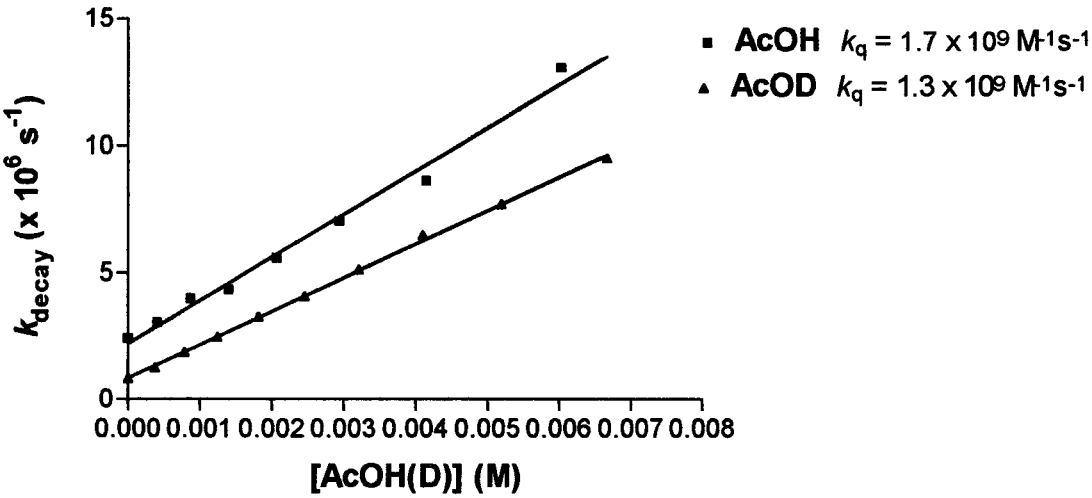

Figure 2.17 Quenching plots of k_{decay} of 7 versus quencher concentration for: Acetic Acid (■) (21.0 °C) and Acetic Acid-d (▲) (21.0 °C) in MeCN at (Tables 2.15-2.16).

Table 2.2 Rate constants for Quenching of Silene 7 with Methanol (MeOH), Methanol-d (MeOD), Ethanol (EtOH), Ethanol-d (EtOD), 2-Propanol (*i*-PrOH), *tert*-Butyl Alcohol (*t*-BuOH), 2,2,2-Trifluoroethanol (TFE), and 1,1,1,3,3,3-Hexafluoroisopropanol (HFIP) in dried oxygenated Hexane Solution at 21.5 - 22.6 °C.[a,b]

Quencher	Temperature (°C)	τ_o (μs)	k_q (x 10^{-9}) (Ms)	R^2	# of Data Points
MeOH	22.0	2.4 ± 1.3	2.1 ± 0.1	0.9971	5
MeOD	21.7	1.7 ± 0.8	1.7 ± 0.1	0.9957	5
EtOH	22.2	1.1 ± 5.3	2.5 ± 0.2	0.9949	6
EtOD	21.5	1.5 ± 0.7	2.1 ± 0.1	0.9961	6
***i*-PrOH**	22.0	1.5 ± 0.8	1.6 ± 0.1	0.9921	7
***t*-BuOH**	22.4	0.9 ± 0.3	0.57 ± 0.04	0.9903	6
TFE	22.6	2.5 ± 1.1	0.21 ± 0.02	0.9882	5
HFIP	22.3	2.1 ± 0.6	0.11 ± 0.01	0.9883	5

a. Errors in the initial lifetime (τ_o) are reported as twice the standard deviation (σ) obtained from (k_o), rate of decay in the absence of any quencher.
b. Errors for the bimolecular quenching rate constant (k_q) are reported as the standard deviation (σ) obtained from the least squares analysis of the data according to equation 1.20.

Table 2.3 Rate constants for Quenching of Silene 7 with Methanol (MeOH), and Methanol-d (MeOD) in dried oxygenated THF Solution at 20.7 - 22.0 °C.[a,b]

Quencher	Temperature (°C)	τ_o (μs)	k_q (x 10^{-9}) (Ms)	R^2	# of Data Points
MeOH	21.3	1.2 ± 0.3	0.59 ± 0.03	0.9923	7
MeOD	22.0	2.2 ± 1.2	0.45 ± 0.03	0.9767	11
MeOH	20.7	0.5 ± 0.4	1.0 ± 0.1	0.9850	7

a. Errors in the initial lifetime (τ_o) are reported as twice the standard deviation (σ) obtained from (k_o), rate of decay in the absence of any quencher.
b. Errors for the bimolecular quenching rate constant (k_q) are reported as the standard deviation (σ) obtained from the least squares analysis of the data according to equation 1.20.

Table 2.4 Rate constants for Quenching of Silene 7 with Water (H_2O), and Deuterium oxide (D_2O) in dried oxygenated Acetonitrile Solution[a,b] at 20.7 - 21.1 °C and 24.6 - 25.5 °C.

Quencher	Temperature (°C)	τ_o (μs)	k_q (x 10^{-9}) (Ms)	R^2	# of Data Points
H_2O	20.7	0.6 ± 0.1	1.8 ± 0.1	0.9944	11
H_2O	20.9	0.29 ± 0.02	3.4 ± 0.1	0.9925	10
H_2O	24.6	0.7 ± 0.1	1.23 ± 0.03	0.9979	10
H_2O	24.7	1.1 ± 0.1	2.5 ± 0.1	0.9960	9
H_2O	25.1	2.9 ± 0.8	0.72 ± 0.04	0.9929	7
H_2O	25.5	1.4 ± 0.1	0.90 ± 0.02	0.9986	7
D_2O	21.1	0.6 ± 0.1	1.19 ± 0.04	0.9967	10

a. Errors in the initial lifetime (τ_o) are reported as twice the standard deviation (σ) obtained from (k_o), rate of decay in the absence of any quencher.
b. Errors for the bimolecular quenching rate constant (k_q) are reported as the standard deviation (σ) obtained from the least squares analysis of the data according to equation 1.20.

Table 2.5 Rate constants for Quenching of Silene 7 with Methanol (MeOH) in dried oxygenated Acetonitrile Solution[a,b] at 20.3 - 22.0 °C, 23.1 - 25.0 °C, and 28.0 - 28.9 °C.

Experiment Number	Temperature (°C)	τ_o (μs)	k_q (x 10^{-9}) (Ms)	R^2	# of Data Points
1	21.1	0.27 ± 0.05	2.4 ± 0.3	0.9688	7
2	22.0	0.33 ± 0.05	1.8 ± 0.1	0.9894	6
3	21.2	0.25 ± 0.03	2 ± 1	0.9941	8
4	20.3	0.23 ± 0.03	2.3 ± 0.1	0.9924	7
5	23.1	0.7 ± 0.2	2.1 ± 0.1	0.9962	12
6	24.6	1.8 ± 1.0	1.8 ± 0.1	0.9954	8
7	23.9	1.2 ± 0.1	1.4 ± 0.2	0.9996	7
8	24.9	1.1 ± 0.2	1.13 ± 0.04	0.9960	8
9	25.0	1.2 ± 0.1	1.17 ± 0.03	0.9981	8
10	28.0	3.8 ± 1.1	1.1 ± 0.3	0.9988	6
11	28.4	2.9 ± 0.5	1.2 ± 0.1	0.9973	4
12	28.9	2.0 ± 0.4	1.41 ± 0.04	0.9980	7
13	28.4	2.5 ± 1.0	1.19 ± 0.04	0.9952	9
14	28.1	1.4 ± 0.5	1.1 ± 0.1	0.9927	6

a. Errors in the initial lifetime (τ_o) are reported as twice the standard deviation (σ) obtained from (k_o), rate of decay in the absence of any quencher.
b. Errors for the bimolecular quenching rate constant (k_q) are reported as the standard deviation (σ) obtained from the least squares analysis of the data according to equation 1.20.

Table 2.6 Rate constants for Quenching of Silene **7** with, Methanol-d (MeOD) in dried oxygenated Acetonitrile Solution[a,b] at 20.6 - 22.0 °C, 23.1 - 25.0 °C, and 28.0 - 28.9 °C.

Experiment Number	Temperature (°C)	τ_o (μs)	k_q (x 10^{-9}) (Ms)	R^2	# of Data Points
1	20.6	1.0 ± 0.2	1.49 ± 0.05	0.9978	6
2	22.0	0.5 ± 0.1	1.42 ± 0.04	0.9974	10
3	23.1	0.12 ± 0.01	1.52 ± 0.03	0.9981	10
4	24.5	1.3 ± 0.1	0.99 ± 0.01	0.9993	9
5	25.0	1.12 ± 0.02	0.90 ± 0.03	0.9979	5
6	28.9	2.0 ± 0.4	1.4 ± 0.1	0.9963	6
7	28.0	2.1 ± 0.2	0.80 ± 0.01	0.9992	9

a. Errors in the initial lifetime (τ_o) are reported as twice the standard deviation (σ) obtained from (k_o), rate of decay in the absence of any quencher.
b. Errors for the bimolecular quenching rate constant (k_q) are reported as the standard deviation (σ) obtained from the least squares analysis of the data according to equation 1.20.

Table 2.7 Rate constants for Quenching of Silene 7 with Ethanol (EtOH) in dried oxygenated Acetonitrile Solution[a,b] at 24.1 -28.7 °C.

Experiment Number	Temperature (°C)	τ_o (μs)	k_q (x 10^{-9}) (Ms)	R^2	# of Data Points
1	24.1	1.0 ± 0.1	1.40 ± 0.03	0.9990	8
2	25.0	0.7 ± 0.1	1.46 ± 0.02	0.9993	9
3	28.3	3 ± 1	1.19 ± 0.02	0.9986	9
4	28.7	2.8 ± 0.5	1.03 ± 0.03	0.9980	7

a. Errors in the initial lifetime (τ_o) are reported as twice the standard deviation (σ) obtained from (k_o), rate of decay in the absence of any quencher.
b. Errors for the bimolecular quenching rate constant (k_q) are reported as the standard deviation (σ) obtained from the least squares analysis of the data according to equation 1.20.

Table 2.8 Rate constants for Quenching of Silene 7 with Ethanol-d (EtOD) in dried oxygenated Acetonitrile Solution[a,b] at 21.0 ± 0.1 °C and 28.5 ± 0.3 °C.

Experiment Number	Temperature (°C)	τ_o (μs)	k_q (x 10^{-9}) (Ms)	R^2	# of Data Points
1	21.0	1.2 ± 0.2	0.99 ± 0.02	0.9980	10
2	28.3	3.0 ± 0.5	0.82 ± 0.02	0.9984	8
3	28.7	1.8 ± 0.4	1.03 ± 0.02	0.9986	9

a. Errors in the initial lifetime (τ_o) are reported as twice the standard deviation (σ) obtained from (k_o), rate of decay in the absence of any quencher.
b. Errors for the bimolecular quenching rate constant (k_q) are reported as the standard deviation (σ) obtained from the least squares analysis of the data according to equation 1.20.

Table 2.9 Rate constants for Quenching of Silene 7 with 2-Propanol (*i*-PrOH) in dried oxygenated Acetonitrile Solution at 24.8 ± 0.2 °C.[a,b]

Experiment Number	Temperature (°C)	τ_o (μs)	k_q (x 10^{-9}) (Ms)	R^2	# of Data Points
1	24.7	5.6 ± 2.8	0.68 ± 0.01	0.9990	9
2	25.0	1.4 ± 0.1	0.76 ± 0.01	0.9986	9

a. Errors in the initial lifetime (τ_o) are reported as twice the standard deviation (σ) obtained from (k_o), rate of decay in the absence of any quencher.
b. Errors for the bimolecular quenching rate constant (k_q) are reported as the standard deviation (σ) obtained from the least squares analysis of the data according to equation 1.20.

Table 2.10 Rate constants for Quenching of Silene 7 with *tert*-Butyl Alcohol (*t*-BuOH) in dried oxygenated Acetonitrile Solution[a,b] at 22.8 - 26.0 °C.

Experiment Number	Temperature (°C)	τ_o (μs)	k_q (x 10^{-9}) (Ms)	R^2	# of Data Points
1	22.8	0.37 ± 0.03	1.11 ± 0.05	0.9933	8
2	23.0	0.8 ± 0.1	0.23 ± 0.01	0.9974	11
3	25.4	1.9 ± 0.2	0.31 ± 0.01	0.9962	9
4	26.0	0.69 ± 0.02	0.31 ± 0.02	0.9968	4

a. Errors in the initial lifetime (τ_o) are reported as twice the standard deviation (σ) obtained from (k_o), rate of decay in the absence of any quencher.
b. Errors for the bimolecular quenching rate constant (k_q) are reported as the standard deviation (σ) obtained from the least squares analysis of the data according to equation 1.20.

Table 2.11 Rate constant for Quenching of Silene 7 with *tert*-Butyl Alcohol-d (*t*-BuOD) in dried oxygenated Acetonitrile Solution[a,b] at 21.0 - 24.6 °C.

Experiment Number	Temperature (°C)	τ_o (μs)	k_q (x 10^{-9}) (Ms)	R^2	# of Data Points
1	21.0	1.1 ± 0.1	0.23 ± 0.01	0.9926	8
2	24.2	1.0 ± 0.1	0.172 ± 0.002	0.9996	10
3	24.6	1.8 ± 0.2	0.138 ± 0.003	0.9984	10

a. Errors in the initial lifetime (τ_o) are reported as twice the standard deviation (σ) obtained from (k_o), rate of decay in the absence of any quencher.
b. Errors for the bimolecular quenching rate constant (k_q) are reported as the standard deviation (σ) obtained from the least squares analysis of the data according to equation 1.20.

Table 2.12 Rate constants for Quenching of Silene 7 with 2,2,2-trifluoroethanol (TFE) in dried oxygenated Acetonitrile Solution[a,b] at 20.8 - 25.2 °C.

Experiment Number	Temperature (°C)	τ_o (μs)	k_q (x 10^{-9}) (Ms)	R^2	# of Data Points
1	20.8	0.9 ± 0.2	1.32 ± 0.03	0.9969	11
2	25.1	3 ± 1	1.7 ± 0.1	0.9929	8
3	25.2	1.0 ± 0.1	1.46 ± 0.03	0.9990	8

a. Errors in the initial lifetime (τ_o) are reported as twice the standard deviation (σ) obtained from (k_o), rate of decay in the absence of any quencher.
b. Errors for the bimolecular quenching rate constant (k_q) are reported as the standard deviation (σ) obtained from the least squares analysis of the data according to equation 1.20.

Table 2.13 Rate constants for Quenching of Silene 7 with 2,2,2-trifluoroethanol-d_3 (TFE-d_3) in dried oxygenated Acetonitrile Solution[a,b] at 21.0 - 25.4 °C.

Experiment Number	Temperature (°C)	τ_o (μs)	k_q (x 10^{-9}) (Ms)	R^2	# of Data Points
1	21.0	1.1 ± 0.1	1.43 ± 0.01	0.9997	10
2	25.4	3.1 ± 1.8	1.24 ± 0.02	0.9989	9

a. Errors in the initial lifetime (τ_o) are reported as twice the standard deviation (σ) obtained from (k_o), rate of decay in the absence of any quencher.
b. Errors for the bimolecular quenching rate constant (k_q) are reported as the standard deviation (σ) obtained from the least squares analysis of the data according to equation 1.20.

Table 2.14 Rate constants for Quenching of Silene 7 with 1,1,1,3,3,3-Hexafluoroisopropanol (HFIP) in dried oxygenated Acetonitrile Solution[a,b] at 23.1 ± 0.1 °C and 24.5 ± 0.1 °C.

Experiment Number	Temperature (°C)	τ_o (μs)	k_q (x 10^{-9}) (Ms)	R^2	# of Data Points
1	23.1	0.66 ± 0.03	1.44 ± 0.02	0.9994	7
2	24.4	0.6 ± 0.1	1.20 ± 0.03	0.9986	8
3	24.6	2.9 ± 0.3	0.928 ± 0.004	1.0000	8

a. Errors in the initial lifetime (τ_o) are reported as twice the standard deviation (σ) obtained from (k_o), rate of decay in the absence of any quencher.
b. Errors for the bimolecular quenching rate constant (k_q) are reported as the standard deviation (σ) obtained from the least squares analysis of the data according to equation 1.20.

Table 2.15 Rate constants for Quenching of Silene 7 with glacial acetic acid (AcOH) in dried oxygenated Acetonitrile Solution[a,b] at 21.0 - 25.6 °C.

Experiment Number	Temperature (°C)	τ_o (μs)	k_q (x 10^{-9}) (Ms)	R^2	# of Data Points
1	21.0	0.4 ± 0.1	1.7 ± 0.1	0.9940	8
2	21.9	0.7 ± 0.1	1.92 ± 0.04	0.9979	11
3	25.6	3 ± 1	1.45 ± 0.02	0.9990	8

a. Errors in the initial lifetime (τ_o) are reported as twice the standard deviation (σ) obtained from (k_o), rate of decay in the absence of any quencher.
b. Errors for the bimolecular quenching rate constant (k_q) are reported as the standard deviation (σ) obtained from the least squares analysis of the data according to equation 1.20.

Table 2.16 Rate constants for Quenching of Silene 7 with glacial acetic acid-d (AcOD) in dried oxygenated Acetonitrile Solution[a,b] at 21.0 - 25.5 °C.

Experiment Number	Temperature (°C)	τ_o (μs)	k_q (x 10^{-9}) (Ms)	R^2	# of Data Points
1	21.0	1.2 ± 0.1	1.32 ± 0.01	0.9995	10
2	25.5	4.6 ± 1.8	1.25 ± 0.02	0.9990	7

a. Errors in the initial lifetime (τ_o) are reported as twice the standard deviation (σ) obtained from (k_o), rate of decay in the absence of any quencher.
b. Errors for the bimolecular quenching rate constant (k_q) are reported as the standard deviation (σ) obtained from the least squares analysis of the data according to equation 1.20.

Table 2.17 Average Rate constants for Quenching of Silene 7 with Water (H_2O), Methanol (MeOH), Ethanol (EtOH), *tert*-Butyl Alcohol (t-BuOH), 2-Propanol (*i*-PrOH), 2,2,2-Trifluoroethanol (TFE), 1,1,1,3,3,3-Hexafluoroisopropanol (HFIP), Acetic Acid (AcOH), and their respective deuterated counterparts in dried oxygenated Acetonitrile Solution at 21 ± 1 °C, 25 ± 1 °C, and 28 ± 1 °C.[a,b]

Quencher	k_q (x 10^{-9} Ms) *21 ± 1 °C*	k_q (x 10^{-9} Ms) *25 ± 1 °C*	k_q (x 10^{-9} Ms) *28 ± 1 °C*
H_2O	3 ± 1[d]	1 ± 1[e]	*f*
D_2O	1.19 ± 0.04[c]	*f*	*f*
MeOH	2.1 ± 0.3[e]	1.5 ± 0.4[e]	1.2 ± 0.1[e]
MeOD	1.48 ± 0.05[e]	0.9 ± 0.1[d]	1.1 ± 0.4[d]
EtOH	*f*	1.43 ± 0.04[d]	1.1 ± 0.1[d]
EtOD	0.99 ± 0.02[c]	*f*	0.92 ± 0.15[d]
***i*-PrOH**	*f*	0.7 ± 0.1[d]	*f*
***t*-BuOH**	0.7 ± 0.6[d]	0.31 ± 0.01[d]	*f*
***t*-BuOD**	0.23 ± 0.01[c]	0.15 ± 0.02[d]	*f*
TFE	1.32 ± 0.03[c]	1.6 ± 0.2[d]	*f*
TFE-d_3	1.43 ± 0.01[c]	1.24 ± 0.02[c]	*f*
HFIP	1.44 ± 0.02[c]	1.1 ± 0.2[d]	*f*
AcOH	1.8 ± 0.1[d]	1.45 ± 0.02[c]	*f*
AcOD	1.32 ± 0.01[c]	1.25 ± 0.02[c]	*f*

a. Temperature at which data were measured is reported as the average temperature for all of the rate constants. The error is reported as the standard deviation (σ) from the mean.

b. Average bimolecular quenching rate constants (k_q) were obtained fromTables 2.4- 2.16 for each of the alcohols.

c. Based on a single determination; quoted error is that in the original value.

d. The average of two (2) determinations; the error is quoted as the standard deviation from the mean.

e. The average of three (3) determinations; the error is quoted as the standard deviation from the mean.

f. No datum collected over this temperature range.

Table 2.18 Determination of Bimolecular Quenching Rate Constants in the Presence of (a) Oxygen and (b) Nitrogen for Methanol (MeOH), Methanol-d (MeOD), and 2,2,2-Trifluoroethanol (TFE) in Acetonitrile at 23.0 ± 1.1 °C.[a]

Quencher	k_q (x 10^{-9}) Ms *O_2 Saturated*	k_q (x 10^{-9}) Ms *N_2 Saturated*
MeOH	1.8 ± 0.1	1.33 ± 0.02
MeOD	0.99 ± 0.03	0.99 ± 0.01
TFE	1.46 ± 0.05	1.2 ± 0.1

a. Errors for the bimolecular quenching rate constant (k_q) are reported as the standard deviation (σ) obtained from the least squares analysis of the data according to equation 1.20.

2.6 Competitive Steady-State Photolysis

Competitive steady-state photolyses were performed in a similar manner to the steady-state photolysis described in Section 2.4 (page 30). In the competition experiment, two quenching agents of equimolar concentration were added to a 0.01 M solution of **6** in cyclohexane, isooctane, or acetonitrile as solvent. The product ratios were estimated using the peak areas of gas chromatography (GC) traces and compared to the corresponding rate ratios calculated from the rate constants measured by *NLFP*. Agreement between the two sets of numbers would confirm that the products generated independently by photolysis do in fact arise directly from the transient being observed in the *NLFP* experiment. Scheme 2.1 indicates the nature of the competitive steady-state experiment.

For quantitative gas chromatographic analyses, the internal standard method was used to generate a calibration curve. A series of standard solutions were prepared by mixing different amounts of stock solutions of alkoxysilane (0.02 M) and dodecane (0.005 M). The calibration curve was generated by plotting the ratios of concentration ([Alkoxysilane]/[Dodecane]) against the ratios of peak areas ($Area^{Alkoxysilane}/Area^{Dodecane}$) between the silyl ether and dodecane. Table 2.19 reports the response factors for the

Scheme 2.1 Competitive Steady-State Photolysis

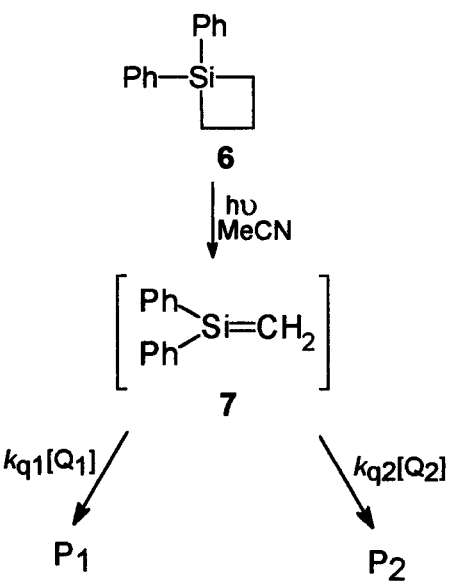

alkoxysilanes with the error. The error represents the standard deviation (σ) of the slope of the calibration curve.

For example, a 0.01 M solution of **6** was prepared in the presence of equimolar concentrations of methanol (0.02 M-0.05 M) and ethanol (0.02 M-0.05 M) in acetonitrile. An internal standard, dodecane, of concentration 0.005 M was added in order to monitor

the percent conversion of **6** upon photolysis. The photolysis was carried to *ca.* 10% conversion of **6**, at which point the photolysate was monitored by GC. GC analysis indicated that two photoproducts were present which are expressed in Table 2.20 as a relative product ratio with respect to methanol. GC/MS verified the identification of the two photoproducts as methoxydiphenylmethylsilane (**34**) and ethoxydiphenylmethylsilane (**35**). Table 2.20 summarizes the results obtained from two independent experiments, competitive steady-state photolysis and transient spectroscopic techniques, respectively.

Table 2.19 Calibration Curve Data For Gas Chromatographic Analysis. Response Factors (F) Calculated For Various Photoproducts.[a,b]

Photoproduct	Relative Response Factor (F)[c]
$Ph_2Si(OCH_3)Me$	1.09 ± 0.04
$Ph_2Si(OCH_2CH_3)Me$	1.0 ± 0.1
$Ph_2Si(OCHMe_2)Me$	0.74 ± 0.03
$Ph_2Si(OCMe_3)Me$	1.15 ± 0.03
$Ph_2Si(OCH_2CF_3)Me$	0.87 ± 0.02
$Ph_2Si(OCH(CF_3)_2)Me$	0.87 ± 0.02

a. Each analysis was performed in triplicate.
b. Errors are reported as the standard deviation (σ) of the slope of the calibration curve.
c. Relative to dodecane.

Table 2.20 Relative Product Ratios with Respect to Methanol Obtained From Competitive Steady-State Photolyses (*ca.* 35 °C)[a] and the corresponding Absolute Rate Constant Ratios Obtained From Transient Spectroscopic Techniques at 21 ± 1 °C, 25 ± 1 °C, and 28 ± 1 °C.[b]

Quencher	$k_{rel}^{c.s.s.}(P_{MeOH}/P_{Quencher})$	$k_{rel}^{n.l.f.p.}(k_{q\ MeOH}/k_{q\ Quencher})$		
		21 ± 1 °C	*25 ± 1 °C*	*28 ± 1 °C*
MeOH	1.00 ± 0.05	1.0 ± 0.2	1.0 ± 0.4	1.0 ± 0.1
EtOH	1.2 ± 0.1	*c*	1.0 ± 0.3	1.1 ± 0.1
***i*-PrOH**	1.5 ± 0.1	*c*	2.1 ± 0.5	*c*
***t*-BuOH**	1.6 ± 0.1	3.1 ± 2.9	4.8 ± 1.3	*c*
TFE	3.8 ± 0.1	1.6 ± 0.2	0.9 ± 0.3	*c*
HFIP	2.6 ± 0.1	1.4 ± 0.2	1.4 ± 0.4	*c*
AcOH	0.9 ± 0.1	1.2 ± 0.2	1.0 ± 0.3	*c*

a. Relative yields at ≤ 10 % conversion of **6**, corrected for GC responses.
b. The absolute rate constant ratios ($k_{rel}^{n.l.f.p.}$) were calculated using the *average* bimolecular rate constants for the alcohols listed in Table 2.17. Errors are reported as the standard deviation (σ) from the mean.
c. No datum collected.

2.6.1 Kinetic Isotope Effect Determination

Kinetic isotope effects are a special type of substituent effect that are very useful in the study of reaction mechanisms.[92,104,105] The kinetic isotope effect is directly dependent upon the shape of the potential-energy surface and can be used to gain insight into the structure of the activated complex.[92,104,105] Table 2.21 (page 65) contains kinetic isotope effect (k_H/k_D) data obtained at 21 ± 1 °C for the addition of methanol and ethanol to 7 in hexane. Table 2.22 contains the KIE's obtained from the *average* absolute bimolecular quenching rate constants (k_q) measured at 21 ± 1, 25 ± 1, and 28 ± 1 °C in acetonitrile (Table 2.17). The KIE's determined from the absolute rate constants (k_q) can be

compared with product ratios determined by competitive steady-state photolyses of solutions containing both the protonated and corresponding deuterated alcohol. For example, a 0.01 M solution of **6** in acetonitrile was photolysed in the presence of 0.05 M MeOH and 0.05 M MeOD to *ca.* 10% conversion. The photoproduct was monitored by GC and GC/MS. GC/MS analysis led effectively to an estimation of the KIE for each alcohol as shown in Table 2.23. Competitive steady-state photolysis (Scheme 2.1) was used in the following manner to calculate the k_H/k_D ratio. Equation 2.7 shows the relationship between the relative rate constants and the ratio of photoproducts formed,

$$(k_H/k_D)\,([MeOH] / [MeOD]) = [Ph_2Si(OCH_3)Me] / [Ph_2Si(OCH_3)CH_2D] \qquad \mathbf{2.7}$$

For competitive steady-state photolysis, both alcohols are equimolar in concentration such that equation 2.7 reduces to equation 2.8,

$$(k_H/k_D) = [Ph_2Si(OCH_3)Me] / [Ph_2Si(OCH_3)CH_2D] \qquad \mathbf{2.8}$$

Thus, the ratio of photoproducts formed is equivalent to the kinetic isotope effect.

By using GC/MS, the ratio of photoproducts (eq. 2.8) was determined using the following steady-state experiments. First, the amount of MeOD present in the photolysis solution containing 0.05 M methanol (MeOH) was determined and expressed as a percentage. Second, the photolysis mixture containing both methanol (MeOH) and methanol-d (MeOD) was analyzed and the ratio of photoproducts was determined in the following manner. The area corresponding to MeOH-photoproduct (228^+) was corrected for the percentage of deuterium present. This amount was subtracted from the MeOD-photoproduct (229^+) yielding the corrected amount of MeOD present in the photolysis mixture. The estimated k_H/k_D value of 1.6 was found to represent the ratio of the actual amount of MeOH to the corrected amount of MeOD as shown in Table 2.23.

Table 2.21 Kinetic Isotope Effect (k_H/k_D) Determination by Transient Spectroscopic Technique for Methanol and Ethanol in Hexane at 22.0 ± 0.5 °C.[a]

Quencher	k_H/k_D
MeOH(D)	1.2 ± 0.1
EtOH(D)	1.2 ± 0.1

a. The bimolecular quenching rate constants (k_q) were taken from Table 2.2. Errors are reported as the standard deviation (σ) obtained from least squares analysis of the data according to equation 1.20.

Table 2.22 Kinetic Isotope Effect (k_H/k_D) Determination by Transient Spectroscopic Technique for Various Alcohols in dried Acetonitrile at 21 ± 1 °C, 25 ± 1 °C, and 28 ± 1 °C.[a]

	Temperature (°C)		
	21 ± 1	*25 ± 1*	*28 ± 1*
Quencher		k_H/k_D	
H_2O/ D_2O	2 ± 1	*b*	*b*
MeOH(D)	1.4 ± 0.2	1.6 ± 0.4	1.1 ± 0.4
EtOH(D)	*b*	*b*	1.2 ± 0.2
BuOH(D)	2.9 ± 2.7	2.1 ± 0.3	*b*
TFE (d_3)	0.92 ± 0.02	1.3 ± 0.2	*b*
AcOH(D)	1.4 ± 0.1	1.2 ± 0.1	*b*

a. The *average* bimolecular quenching rate constants (k_q) were taken from Table 2.17 for the various alcohols studied at three temperature ranges. Errors are reported as the standard deviation (σ) from the mean.
b. No data collected over this temperature range.

Table 2.23 Kinetic Isotope Effect Determination by GC/MS From Competitive Steady-State Photolysis of Various Alcohols in dried Acetonitrile at approximately 35.0 ± 1.0 °C.[a]

Quencher	k_H/k_D
MeOH/ MeOD	1.6
EtOH/ EtOD	1.7
***t*-BuOH/ *t*-BuOD**	2.8
TFE/ TFE-d_3	3.0

a. Error is considered to be *ca.* 10 %.

CHAPTER 3

DISCUSSION

3.1 Synthesis of 6

The synthesis of **6** as shown in equation 2.1[98] resulted in a crude yield of 90%. As previously mentioned, biphenyl was present in minute amounts and upon photolysis biphenyl triplet was generated. The biphenyl triplet absorbs at 360 nm[102] and has a reasonably large extinction coefficient (ε_{max} = 3700 $M^{-1}cm^{-1}$)[102], so that overlap with the silene absorption at 325 nm can interfere with the characterization of the reactivity of **7** directly. Compound **6** was purified by vacuum distillation in order to remove the trace quantities of biphenyl. The final yield of **6** (99.9% pure by GC) was 82%. In order to further minimize complications from trace amounts of biphenyl (< 0.1%), the sample was purged with a stream of extra dry oxygen. Since oxygen reacts with **7** slowly, $k_q \approx 5 \times 10^6 M^{-1}s^{-1}$ [86] but is an efficient triplet quencher,[102] it is a suitable trapping agent for biphenyl triplets[102] without affecting the lifetime of the simple silene.

3.2 Thermal Stability of 6 in Alcohols

The thermal stability of **6** towards the various alcohols studied as silene traps was analyzed. The results indicated that **6** is stable toward each of the alcohols studied for extended periods of time (>72 hours) at room temperature. This can be compared with 1,1,2-triphenylsilacyclobutane (**19**)[86] which was found to undergo a dark reaction with methanol in acetonitrile over a period of several hours, yielding the acyclic silyl methyl ether (**20**) as shown in equation 1.12.[86]

3.3 Steady-State Photolysis of 6 in the Presence of Alcohols

The photolysis of 1,1-diphenylsilacyclobutane, **6**, in the presence of alcohols leads to the formation of a single photoproduct consistent with alcohol addition to the corresponding silene, **7**. It is of importance to note that the photolysis of **7** in an anhydrous solvent such as isooctane results in the formation of a single photoproduct, whereas photolysis in acetonitrile leads to the formation of two photoproducts. The minor product is assigned to the reaction product of **7** with water (eq. 2.4; page 32). The relative yield of **9** varied directly with the amount of water present in the solvent. Water is present in HPLC grade acetonitrile at concentrations of *ca.* 16 mM.[100] After distillation from calcium hydride,[103] the level of water was estimated to be *ca.* 0.8 mM using equation 1.20[93,94] and substituting kinetic data obtained for quenching of **7** by water (Table 2.4). Distillation from calcium hydride followed by passage through activated alumina[103] reduced the water content to approximately 0.3 mM. Photolysis of **6** in rigorously dried MeCN containing 0.05 M methanol resulted in the formation of **8** as the only detectable product.

Steady-state photolysis of isooctane solutions of **6** containing 0.01 M methanol to *ca.* 10% conversion generated a single photoproduct based on GC and GC/MS analyses, consistent with alcohol addition to silene **7** (eq. 2.2; page 31).

3.4 Nanosecond Laser Flash Photolysis of 6

3.4.1 Characterization of 7 by NLFP

Nanosecond laser flash photolysis of **6** in acetonitrile, isooctane, and hexane generates transient absorptions which show a maximum centered around 325 nm, as illustrated in Figures 2.6(b), 2.7(b), and 2.8(b), respectively. This transient species has been assigned as 1,1-diphenylsilene (**7**) based on the location of the ultraviolet absorption maximum[26,27a,27b,41,42,81,83] and the reactivity towards known silene traps.[77,86]

An absorption maximum centered around 325 nm is a reasonable assignment for the ultraviolet spectrum of **7**, which can be demonstrated by comparing the UV absorption spectra of other silenes with their respective hydrocarbon analogues. For example, the UV spectrum of the parent silene, silaethene, at 10 K shows a maximum centered at 258 nm,[42] while that of ethylene occurs at 165 nm.[41] Thus, substitution of silicon for carbon results in a ~ 90 nm red-shift in the absorption maximum in this case. The thermal generation of 1,1-dimethylsilene **2** in equation 1.1 allowed the measurement of the ultraviolet spectrum of the transient **2** which showed a maximum centered around 244 nm.[41] This can be compared with the carbon analogue 1,1-dimethylethylene, which shows a maximum located at 180 nm,[41] corresponding to a silicon - induced shift of ~ 65 nm. The ultraviolet absorption spectrum of 1,1-diphenylethylene exhibits an absorption maximum at 250 nm;[41] thus, a λ_{max} of 325 nm for **7** is reasonable, given the above data for silaethene and **2**.

3.4.2 Verification of the Identity of the Transient as Silene 7

It has been rationalized that the transient spectrum observed in *NLFP* experiments with **6** indicates that it is consistent with that expected for 1,1-diphenylsilene (**7**). Other pieces of evidence also support this assignment. Firstly, the same spectrum has been reported in *NLFP* studies using different photochemical precursors of **7** such as 1,1,2-triphenylsilacyclobutane (**19**)[86] and methylpentaphenyldisilane.[77] Also, the rate constants for reaction of the present transient with various silene traps such as methanol, acetone, oxygen and dienes are in good agreement with those reported using the other precursors.

The previously reported precursors of **7** were originally identified as such based on product studies; the products observed upon steady state photolysis of **6**, **19**, and $Ph_3SiSiPh_2Me$ in the presence of methanol or acetone are consistent with the intermediacy of this species. This work demonstrates that the transient reacts with various other alcohols, water and acetic acid through *NLFP* studies. Steady state photolysis experiments indicate that the expected reaction products of these reagents with **6** are indeed formed in high yields (Table 2.1). Comparison of the relative rate constants (for reaction of the transient with pairs of alcohols) to the ratios of the corresponding product yields in steady state photolysis experiments was used to further test the assignment of **7**. To a first approximation, if the transient observed by *NLFP* is the same as that being trapped in the steady state experiment (Scheme 2.1; page 61), then the product ratio obtained from photolysis in the presence of two trapping agents of known concentrations ($k_{rel}^{css} = P_{MeOH}/ P_{ROH}$) should be identical to the ratio of the absolute rate constants for reaction of the transient with the two reagents ($k_{rel}^{nlfp} = P_{MeOH}/ P_{ROH}$) as shown in equation 2.8 (page 64). A comparison of these ratios for each of the hydroxylic trapping agents studied is shown in Table 2.20. Agreement between the two values is observed only for MeOH/EtOH, MeOH/*i*-PrOH, and MeOH/HOAc. For *t*-BuOH, k_{rel}^{css} is significantly

higher than k_{rel}^{nlfp} while the opposite is trend is observed for TFE and HFIP. These discrepancies are not believed to be due to a misassignment of the structure of the transient observed in the *NLFP* experiments. These may be due to experimental problems such as inaccurate determination of the absolute concentrations of the trapping reagents in the photolysis solutions or in the stock solutions used for determination of the GC response factors. In most cases, the solutions were made by adding microlitre quantities of neat trap to known volumes of solvent. Higher accuracy could be obtained by weight measurements. This possible source of error is more than likely an assignable cause for the poor reproducibilities in the absolute rate constants (k_q) reported in Tables 2.2-2.18. A second problem concerns the conditions under which the steady state photolysis experiments were carried out, as these were significantly different than those employed in the *NLFP* experiments. That is, both the temperature and the total alcohol concentrations were higher in the steady state experiments. Given the complexity of the previously proposed mechanism for addition of alcohols to silenes (Chapter 1, Section 1.4.3), the higher concentrations used in the steady state experiments may result in substantial deviations of k_{rel}^{css} from the expected values. At higher alcohol concentrations attention must be given to the possible *inter*molecular proton transfer where the excess alcohol acts as a base to deprotonate the complex. In the case where two alcohols are present of different basicities, this may in fact lead to different product ratios than predicted by k_{rel}^{nlfp} which were measured at much lower alcohol concentrations.

3.5 Mechanism of Alcohol Addition to the Silicon-Carbon Double Bond

Leigh and Sluggett reported a detailed mechanistic study regarding the stepwise addition of alcohols to aryldisilane-derived silatrienes **12** using nanosecond laser flash and

steady-state photolysis techniques. This complements the work reported by Sakurai and coworkers using a cyclic silene **28** as introduced in Chapter 1, Section 1.4.3.[77-83] Ab initio calculations by Nagase and coworkers[96,97] confirms the high reactivity of silaethenes towards nucleophiles and suggests that the reaction will occur in a stepwise manner. The following will discuss the predictions of the reactivity of the simple silene **7** based on previous studies of alcohol addition to silenes followed by the experimental data obtained from this preliminary study outlined in this thesis.

3.5.1 Predictions of the Reactivity of 7 Towards Alcohols

Predictions with respect to the reactivity of a simple silene were proposed based on the information (Chapter 1, Section 1.4.3, page 12) regarding the alcohol addition to a conjugated silene **12**,[77-83] cyclic silene **28**,[88] and ab initio calculations.[96,97] The mechanism of alcohol addition to silatriene **12** was proposed to be stepwise (Scheme 1.7) based on the quadratic dependence of k_{decay} on the alcohol concentration, the fact that k_{decay} is more sensitive to nucleophilicity than acidity and the primary kinetic isotope effect.[77-83] Ab initio calculations[96,97] appear to also support a stepwise nucleophilic addition mechanism for the addition of water to silaethene.

The structure of the alcohol-silene complex which would be involved in the addition of alcohols to **7** is shown in Scheme 3.1. That such a complex is probably involved is indicated by the large spectral shift observed for **7** in THF, a solvent which is known to form complexes with other silenes. The THF-**7** complex is analogous to the ROH-**7** complex, except that it has no acidic proton to transfer and proceed to product.

Scheme 3.1 1,1-Diphenylsilene- Alcohol Complex

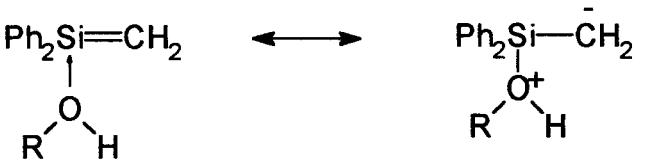

The localized charge at the silenic carbon in the ROH-7 complex should render it less stable than the silatriene-alcohol complex[82] due to the lack of resonance stabilization. The lack of stability should result in the complex being hotter towards *intra*complex proton transfer. This should result in an increased relative contribution from the reaction pathway which is overall first order in [ROH], and result in a linear plot of k_{decay} vs. [ROH] at low alcohol concentrations. This is indeed what is observed.

3.5.2 Reactivity of 7 towards Different Alcohols

Previously, it was discussed (Section 3.5.1) that the linear dependence of k_{decay} on [ROH] suggests that at low alcohol concentrations (< 0.01 M), the mechanism for addition of alcohols to **7** is simpler than that proposed for the more highly conjugated silenes reported by Leigh and Sluggett.[77-83] With respect to **7** the results suggest that the pathway which is bimolecular in [ROH] is relatively unimportant at low [ROH] such that the mechanism for alcohol addition can be approximated as shown in Scheme 3.2. If complex formation (*i.e.* the first step in Scheme 3.2) is rate-determining, then the second-order quenching rate constant (k_q) should show a secondary deuterium kinetic isotope effect ($k_H/k_D \leq 1.2$). But, if complex formation is fast and reversible and proton transfer is rate-determining as shown in Scheme 3.2 then a primary KIE would be expected. Table 2.22 lists the kinetic isotope effect (k_H/k_D) data which suggest that the

Scheme 3.2 Mechanism of Alcohol Addition to 7

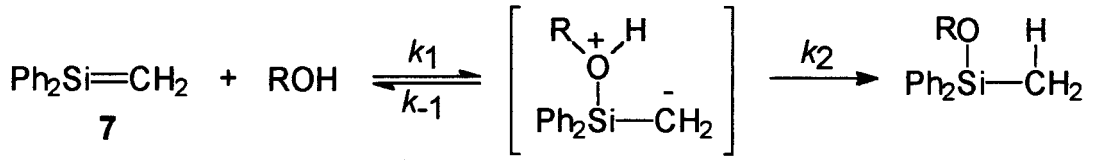

latter is the case for water and non-fluorinated alcohols, although the large errors in the k_H/k_D values make this conclusion tentative.

The rate constants for reaction of **7** with water and non-fluorinated alcohols were found to be roughly an order of magnitude larger and follow a similar trend with alcohol structure as those reported for silatriene **12**.[77-83] But, the rate constants are still an order of magnitude lower than the diffusion-controlled limit of ~ 10^{10} $M^{-1}s^{-1}$ in MeCN[102] such that some sensitivity to alcohol structure is expected. At this point, it is difficult to rationalize the variation in k throughout the series since the overall rate constant ($k_{overall}$) as shown in equation 3.1 is a function of the rates of both formation and collapse of the silene-alcohol complex (Scheme 3.2).

$$k_{overall} \approx (k_1 k_2 / (k_{-1} + k_2)) \qquad \textbf{3.1}$$

The acidic traps TFE, HFIP and HOAc give rise to rate constants similar to that of methanol but the KIE's are significantly lower and indistinguishable from unity. If complex formation is the rate-determining step then the absence of a KIE would be expected. This seems quite reasonable since the higher acidity of these reagents would increase k_2 from its value for methanol whereas the lower nucleophilicities would lower k_1. It is difficult to rationalize the similarities in the overall rate constants for these compounds and the non-acidic alcohols due to the complex nature of the reaction mechanism;

variations in the magnitude of k_1 may be offset by opposing variations in k_2 throughout the series.

Also, it was observed throughout the rate data (Table 2.17) that the magnitude of the bimolecular quenching rate constants (k_q) measured over a 7 °C temperature range appear to show an inverse Arrhenius temperature dependence.[92,104,105] Given the low accuracy in the rate constants and the very small temperature range, it is difficult to place much significance on this trend. If it is real, however, it would provide additional evidence supporting the stepwise mechanism for the reaction of **7** with alcohols. The Arrhenius dependence of the rate constants for these reactions clearly needs to be studied in greater detail.

3.5.3 Sources of Error

Additional sources of error that led to the discrepancies between the C.S.S. and *NLFP* studies will now be reviewed in more detail. A possible source of error could be generated from the preparation and addition of the quenchers to the precursor. The experimental error could be a result of using two separate methods in which the quencher solutions were prepared which include mass and syringe. The addition of the quencher to the flow reservoir is probably a major source of error since one is introducing such a small volume of quencher (μL) to a 100 mL graduated flow reservoir that is being purged with oxygen. This could lead to the evaporation of quencher and inadequate mixing into the solution, thus introducing errors in the alcohol concentrations. This type of error can be controlled through experimental design. For example, a syringe pump would be of assistance in accurately delivering a small volume directly to the solution contained in the large flow reservoir such that evaporation would not be a problem.

CHAPTER 4

SUMMARY AND CONCLUSIONS

4.1 Contributions of the Study

Photolysis of 1,1-diphenylsilacyclobutane (**6**) in solution yields a reactive intermediate 1,1-diphenylsilene (**7**). Rate constants for the reaction of **7** with water, methanol, ethanol, 2-propanol, *tert*-butyl alcohol, 2,2,2-trifluoroethanol, 1,1,1,3,3,3-hexafluoroisopropanol, and acetic acid have been determined.

The preliminary results gathered from this thesis suggests (Section 3.5.2, page 73) that the mechanism (Scheme 3.2) for addition of alcohols to **7** is simpler than proposed for the more highly conjugated silene (**12**).[77-83]

Therefore, this study has led to the *direct* detection of **7** using nanosecond laser flash photolysis techniques. Moreover, this study has contributed to the theory and practical experiments regarding the reactivity of simple silenes.

4.2 Future Work

Related work which is currently underway in our laboratory[106] includes the synthesis of several para-substituted diphenylsilacyclobutanes in order to further study the effects of structure-reactivity relationships when quenching with alcohols in order to elucidate the mechanistic details of alcohol addition to **7**. To date, it seems as though preliminary kinetic data for the quenching of the following substituted silacyclobutanes where (X= p-CH_3 and p-CF_3) with methanol contribute along with the parent silacyclobutane in the formation of a three point Hammett Plot whose slope (ρ) is 0.5 ± 0.3. The slightly

postive nature of the ρ-value implies that the transition state is negatively charged and that the first step in the reaction mechanism is rate-determining in nature.

Quantum yield determinations for the reaction of **6** with various alcohols with the parent and substituted silacyclobutanes would be a tedious but nevertheless a worthwhile investigation in order to get an idea of the efficiency of the formation of the transient.

The measurement of fluorescent lifetimes would also be beneficial in order to justify the quantum yield measurements.

Determination of activation energies (E_a) over a larger temperature range (-35 to 60°C) for the quenching of **7** with weakly acidic and acidic alcohols is necessary in order to obtain the full understanding of the measured rate constants using nanosecond laser flash photolysis techniques. Preliminary experiments merely looked at the effect of temperature on the reaction rate over a 9 °C range. At this point, an apparatus such as a stir flow reactor[107] would definitely be useful in the measurement of the Arrhenius parameters.

CHAPTER 5

EXPERIMENTAL

5.1 General

^{1}H NMR spectra were recorded on Bruker AC 300 (300 MHz), AC 200 (200 MHz), or Varian EM 390 (90 MHz) spectrometers in deuterated chloroform solution and are reported in parts per million (δ) downfield from tetramethylsilane using the residual solvent proton resonances as the internal standard. ^{13}C NMR spectra were recorded on the AC 300 (75.5 MHz) or AC 200 (50.3 MHz) spectrometers. ^{29}Si NMR spectra were recorded on the AC 300 (59.6 MHz) spectrometer in a solution of 0.02 M $Cr(acac)_3$ in deuterated chloroform. Ultraviolet absorption spectra were recorded on a Hewlett-Packard HP8451 UV spectrometer or a Perkin-Elmer Lambda 9 spectrometer interfaced to an IBM-PS2 microcomputer. High resolution desorption electron impact (DEI) mass spectra were recorded on a VG ZAB-E mass spectrometer. Exact masses were determined for the molecular ion (M^+) employing a mass of 12.0000 for carbon. Infrared spectra on purified samples dissolved in deuteriochloroform were recorded on a Bio-Rad FTS-40 FTIR spectrometer and are reported in wavenumbers (cm^{-1}). Gas chromatographic analyses were carried out using a Hewlett-Packard 5890 gas chromatograph equipped with a flame ionization detector, a Hewlett-Packard 3396A recording integrator and one of the following fused silica capillary columns: (a) 5 m x 0.53 mm HP-1; Hewlett-Packard, Inc. and (b) 15 m x 0.20 mm DB-1; Chromatographic Specialties, Inc.. A conventional heated splitless injector port (210-230 °C) was used with both columns, (a) and (b), respectively. Semi-preparative VPC separations employed a Varian 3300 gas chromatograph equipped with a thermal conductivity detector and a

6' x 0.25 " stainless steel OV-101 packed column, Chromatographic Specialties Incorporated. GC/MS analyses were carried out using a Hewlett-Packard 5890 gas chromatograph equipped with a HP-5971A mass selective detector and a DB-1 capillary column (12m x 0.2mm ; Chromatographic Specialties, Inc). GC/FTIR analyses employed a Hewlett-Packard 5890 gas chromatograph equipped with an HP-1 megabore capillary column (5 m x 0.5 mm; Hewlett-Packard, Inc.) and a Bio-Rad GC/32 interface to the Bio-Rad FTS-40 FT-IR spectrometer. Preparative steady state photolysis equipment consisted of using a Rayonet photochemical reactor equipped with a merry-go-round and one to eleven RPR - 254 (254 nm) lamps.

5.2 Commercial Solvents and Reagents

Water (Caledon HPLC), deuterium oxide (MSD Isotopes), acetonitrile-d_3 (Isotec), chloroform-d (MSD Isotopes; Isotec), glacial acetic acid (Fisher Reagent), acetic acid-d (Aldrich), methanol-d (Aldrich), 1,1-dichorosilacyclobutane (Huls America), and chlorodiphenylmethylsilane (Aldrich) were used as received from the suppliers. Acetonitrile (BDH Reagent or Caledon Reagent) was refluxed over calcium hydride (Fisher) for several days and distilled under dry nitrogen. The solvent was then further dried by passage through a 1 x 6 inch column of neutral alumina (Fisher) which had been activated by heating at 320 °C for 10 hours under high vacuum. Methanol (Baker Reagent), and absolute ethanol were predried with calcium hydride, distilled from magnesium under nitrogen, and stored over molecular sieves (3Å). *tert*-butyl alcohol (Fisher Reagent) and 2-propanol (Caledon Reagent) were predried with calcium oxide, distilled from calcium hydride under nitrogen, and stored over molecular sieves (4Å). Cyclohexane (BDH Reagent; Baker HPLC Reagent), 2,2,4-trimethylpentane (Caledon

Reagent), 2,2,2-trifluoroethanol (Aldrich NMR Grade), and 1,1,1,3,3,3-hexafluoroisopropanol (Lancaster) were distilled before use.

5.3 Preparation and Characterization of Compounds

1,1-diphenylsilacyclobutane (**6**) was synthesized and exhibited a boiling point and spectral data which agreed with the literature.[98] Methoxymethyldiphenylsilane[99,99a] (**34**) and ethoxymethyldiphenylsilane[99b,99c] (**35**) were synthesized by reaction of chloromethyl-diphenylsilane and the appropriate alcohol. Bulkier alkoxysilanes such as *t*-butoxy-methyldiphenylsilane[99a] (**37**), isopropoxymethyldiphenylsilane[99d] (**36**), trifluorooxy-methyldiphenylsilane (**38**), and hexafluoroisopropoxymethyldiphenylsilane (**39**) were synthesized by photolysis of **6** (0.02 M) in isooctane containing the alcohol (0.1 M) of choice to *ca.* 65 % conversion as described in (Section 2.4; page 30). The alkoxysilanes were isolated and purified by preparative gas chromatography followed by character-ization by ^{1}H-NMR, ^{13}C-NMR, ^{29}Si-NMR, GC, GC/MS, FT-IR, UV, and mass spectrometry.

1,1-diphenylsilacyclobutane (**6**).[98] Bromobenzene (12.1 g, 70 mmol) was dissolved in dry diethyl ether (10 mL) and placed in a 100 mL addition funnel. To this was added 1,1-dichlorosilacyclobutane (4.9 g, 30 mmol) in diethyl ether (10 mL). The solution was added dropwise to a 250 mL round bottom flask containing magnesium turnings (2.1 g, 90 mmol) in diethyl ether (10 mL) equipped with a reflux condenser, nitrogen inlet, and magnetic stirrer over a 2 hour period. After the addition was complete the resulting solution was refluxed gently for two hours. The reaction mixture was cooled and filtered via gravity into a 500 mL separatory funnel. The salts were washed several times with diethyl ether. The filtrate was then extracted three times with 25 mL portions

of saturated aqueous ammonium chloride. The ether-layer was then washed three times with 25 mL portions of distilled water. The ether extracts were combined and dried with anhydrous magnesium sulphate and the solvent was removed using a rotary evaporator, yielding a light yellow viscous liquid. The resulting liquid was distilled at 80°C under reduced pressure (0.05 mm Hg) several times to yield 1,1-diphenylsilacyclobutane as a clear colourless oil (6.4 g, 30 mmol, 82%).

b.p. = 80°C (0.05 mm Hg).

^{1}H NMR ($CDCl_3$), 200 MHz): δ = 1.50 (t, 4H, Si $\mathbf{CH_2CH_2CH_2}$)

δ = 2.24 (p, 2H, $SiCH_2\mathbf{CH_2}CH_2$), δ = 7.4-7.6 (m, 10H, **SiPh**).

^{13}C NMR ($CDCl_3$, 50.3 MHz): δ = 13.8, 18.3, 127.9, 129.6, 134.5, 136.4.

^{29} Si NMR ($CDCl_3$, 59.6 MHz): δ = 6.78.

IR ($CDCl_3$): 3080 (m), 2990 (m), 2850 (m), 1490 (m), 1420 (s), 1390 (m), 1300 (m), 1250 (m), 1200 (m), 1100 (s), 1000 (m), 900 (s), 850 (s), 790 (s).

GC/MS: *m/z* (I) = 224 (15), 196 (100), 181 (97), 165 (24), 105 (97), 79 (27), 53 (48).

MS: *m/z* (I) = 224(7), 196 (100), 181 (53), 165 (7),146 (7),105 (43), 79 (6), 53 (7).

UV (cyclohexane): λ_{max} = 260 nm; ε_{248} = 910 $M^{-1}cm^{-1}$.

Exact mass: calculated for $C_{15}H_{16}Si$, *m/z* 224.1021; found, 224.1014.

Photoproduct Identification. Preparative Photolysis of 6 in Methanolic Isooctane to Isolate the Corresponding Alkoxysilane.

A 10 mL 0.02 M solution of **6** in isooctane containing 0.1 M methanol was irradiated (254 nm, 11 lamps, 15 minutes) to *ca.* 65 % conversion. The solvent from the 10 mL photolytic sample was removed by use of a steam bath. The photolysate was then diluted with 500 μL of pentane. A 50 μL aliquot was then injected into the preparative GC and separated . The purity of the collected photolysate was then analyzed by use of the GC

(FID). The pure (99.9%) by GC and GC/MS alkoxysilane was fully characterized by ^{1}H NMR, ^{13}C NMR, ^{29}Si NMR, FT-IR, UV, mass spectrometry and by coinjection with the photolysate.

***Methoxymethyldiphenylsilane*(34)**:[99,99a] In a round bottom flask (25 mL) equipped with a reflux condenser, nitrogen inlet, and magnetic stirrer, methyldiphenylchlorosilane (2.6 g, 11.1 mmol) was dissolved in dry diethyl ether (13.6 mL). To this was added an ether solution containing MeOH (0.68 g, 21.2 mmol) and pyridine (1.27 g, 16 mmol). After the addition, the solution was stirred for one hour. After one hour, the insoluble pyridine hydrochloride was filtered via gravity. The solvent and excess methanol were removed on the rotary evaporator which left behind a clear colourless liquid. The liquid was distilled at 149 °C under reduced pressure (8 mm Hg) to yield **34** as a clear colourless liquid (2.1 g, 9.2 mmol, 83%).

b.p. = 149 °C (8.0 mm Hg).

^{1}H NMR ($CDCl_3$, 200 MHz): δ = 0.63 (s, 3H, SiC**H**$_3$), 3.53 (s, 3H, SiOC**H**$_3$), 7.35-7.54 (m, 10H, Si**Ph**).

^{13}C NMR ($CDCl_3$, 50.3 MHz): δ = -3.6, 51.2, 127.9, 129.8, 134.3, 135.6.

^{29}Si NMR ($CDCl_3$, 59.6 Mhz): δ = -0.90.

IR ($CDCl_3$): 3080 (m), 2990 (s), 2825 (s), 1600 (m), 1420 (m), 1250 (s), 1200 (s), 1100 (s), 1080 (s).

GC/MS: *m/z* (I) = 228 (16), 213 (100), 183 (27),151 (5),121 (13), 105 (10), 91 (5), 77 (3), 59 (8).

MS: *m/z* (I) = 228 (9), 213 (100), 183 (27), 151 (9), 121 (12), 105 (11), 91 (7), 77 (3), 59 (10).

UV (cyclohexane): λ_{max} = 260 nm.

Exact mass: calculated for $C_{14}H_{16}OSi$, *m/z* 228.0974; found, 228.0970.

***Ethoxymethyldiphenylsilane* (35)**:[99b,99c]

b.p. = 152°C (8.0 mm Hg).

^{1}H NMR ($CDCl_3$, 200 MHz): δ = 0.62 (s, 3H, $SiCH_3$), δ = 1.20 (t, 3H, $SiOCH_2CH_3$, J = 8.5 Hz), δ = 3.76 (q, 2H, $SiOCH_2CH_3$, J = 8.4 Hz), δ = 7.35-7.57 (m, 10H, Si**Ph**).

^{13}C NMR ($CDCl_3$, 50.3 MHz): δ = -2.94, 18.4, 59.2, 127.8, 129.7, 134.3, 136.2.

IR ($CDCl_3$): 3080 (m), 2990 (s), 2970 (m), 1600 (m), 1465 (s), 1400 (m), 1275 (s), 1120 (s), 1080 (s), 950 (m), 790 (s).

GC/MS: *m/z* (I) = 242 (9), 227 (100), 197 (26), 183 (72), 165 (12), 152(9), 137 (16), 121 (20), 105 (24), 91 (13), 77(19), 51 (11).

MS: *m/z* (I) = 242 (8), 227 (100), 197 (12), 183 (65), 165 (10), 164 (12), 137 (11), 121 (13), 105 (12), 91 (5), 77 (11), 47 (13).

UV (cyclohexane): λ_{max} = 260 nm.

Exact mass: calculated for $C_{15}H_{18}OSi$, *m/z* 242.1129 ; found, 242.1127.

***t-Butoxymethyldiphenylsilane* (37)**:[99a]

^{1}H NMR ($CDCl_3$, 200 MHz): δ = 0.66 (s, 3H, $SiCH_3$), δ = 1.25 (s, 9H, $SiOC(CH_3)_3$), δ = 7.33-7.58 (m, 10H, Si**Ph**).

^{13}C NMR ($CDCl_3$, 50.3 MHz): δ = 0.06, 14.0, 32.1, 127.6, 129.3, 134.2, 136.2.

IR ($CDCl_3$): 3100 (m), 2980 (m), 2900 (m), 1600 (m), 1490 (m), 1420 (m), 1390 (m), 1300 (m), 1210 (s), 1120 (s), 1050 (s), 860 (m), 790 (s).

GC/MS: *m/z* (I) = 270 (5), 255 (48), 199 (100), 181 (13), 165 (7), 137 (18), 105 (14), 91 (6), 77 (7), 51 (3).

MS: *m/z* (I) = 270 (4), 255 (44), 199 (100), 181 (8), 137 (25), 105 (9), 77 (6), 47 (6).

UV (cyclohexane): λ_{max} = 260 nm.

Exact mass: calculated for $C_{17}H_{22}OSi$, *m/z* 270.1452 ; found, 270.1440.

***i-Propoxymethyldiphenylsilane* (36)**:[99d]

^{1}H NMR ($CDCl_3$, 200 MHz): δ = 0.615 (s, 3H, SiC**H**$_3$), δ = 1.19 (d, 6H, SiOCH(C**H**$_3$)$_2$, J = 7.2 Hz), δ = 4.08 (p, 1H, SiOC**H**(CH$_3$)$_2$, J = 7.3 Hz).

^{13}C NMR ($CDCl_3$, 50.3MHz): δ = -2.8, 25.7, 65.8, 127.8, 129.6, 134.2, 136.8.

IR ($CDCl_3$): 3080 (m), 2990 (s), 2970 (m), 1600 (m), 1420 (m), 1390 (m), 1250 (m), 1190 (m), 1120 (s), 1000 (s), 790 (s).

GC/MS: *m/z* (I) = 256(2),241(66),199(100), 178(20), 165(10),137(34), 123(10), 105(27), 91(10), 77(15), 51(8).

MS: *m/z* (I) = 256 (3), 241 (92), 199 (100), 183 (29), 178 (30), 137 (36), 105 (13), 91 (5), 77 (13), 47 (11).

UV (cyclohexane): λ_{max} = 260 nm.

Exact mass: calculated for $C_{16}H_{20}OSi$, *m/z* 256.1286 ; found, 256.1283.

***Trifluoroethoxymethyldiphenylsilane* (38)**:

^{1}H NMR ($CDCl_3$, 200 MHz): δ = 0.69 (s, 3H, SiC**H**$_3$), δ = 3.95 (q, 2H, SiOC**H**$_2$CF$_3$, J = 10.3 Hz), δ = 7.35-7.59 (m, 10H, Si**Ph**).

^{13}C NMR ($CDCl_3$, 50.3 MHz): δ = -3.8, 26.9, 61.4, 128.1, 130.4, 134.3, 136.2.

IR ($CDCl_3$): 3100 (m), 3050 (m), 2980 (m), 1600 (m), 1420 (m), 1300 (s), 1190 (s), 1110 (s), 980 (s), 820 (m), 790 (s).

GC/MS: *m/z* (I) = 296 (37), 143 (25), 139 (20), 91 (100), 77 (10), 47 (7).

MS: *m/z* (I) = 296 (18), 201 (38), 143 (20), 139 (17), 91 (100), 77 (10), 47 (12).

UV (cyclohexane): λ_{max} = 260 nm.

Exact mass: calculated for $C_{15}H_{15}OSiF_3$, *m/z* 296.0844 ; found, 296.0844.

***Hexafluoroisopropoxymethyldiphenylsilane* (39)**:

^{1}H NMR ($CDCl_3$, 200 MHz): δ = 0.73 (s, 3H, $SiCH_3$), δ = 4.18 (p, 1H, $SiOCH(CF_3)_2$, J = 7.0 Hz), δ = 7.42-7.57 (m, 10H, Si**Ph**).

^{13}C NMR ($CDCl_3$, 50.3 MHz): δ = -2, 72, 128.2, 130.8, 134.5, 136.8.

IR ($CDCl_3$): 3100 (m), 3050 (m), 2980 (m), 1600 (m), 1420 (m), 1390 (m), 1300 (s), 1250 (s), 1210 (s), 1100 (s), 860 (s), 840 (m), 790 (s).

GC/MS: *m/z* (I) = 364 (73), 251 (9), 243 (5), 227 (10), 201 (99), 139 (63), 127 (100), 109 (31), 91 (26), 77 (22), 51 (19).

MS: *m/z* (I) = 364 (37), 251 (3), 227 (6), 201(87), 159 (20), 139 (36), 127 (100), 109 (17), 105 (15), 91 (18), 81 (11), 77 (13), 51 (20), 47 (18).

UV (cyclohexane): λ_{max} = 260 nm.

Exact mass: calculated for $C_{16}H_{14}OSiF_6$, *m/z* 364.0709 ; found, 364.0718.

5.4 Steady-State Photolysis

5.4.1 General Methods

Steady-state photolysis experiments were carried out in a Rayonet photochemical reactor equipped with a merry-go-round and one to eleven RPR-254 (254 nm) lamps. Photolysis solutions were contained in 5 x 75 mm, 9 x 100 mm quartz tubes sealed with rubber septa. Chemical yields and percent conversions were determined by GC by use of an internal integration standard (dodecane) relative to the disapppearence of the starting silane. The response of the FID detector was calibrated relative to the internal standard by the construction of calibration curves for the photoproducts. The photoproducts were identified by a combination of ^{1}H NMR spectroscopy, GC/MS, GC/FTIR, and/or by GC coinjection of the photolysates with authentic samples. The following section describes a typical experiment of this type. The compounds studied: ethanol, *t*-butyl alcohol, 2-

propanol, 2,2,2-trifluoroethanol, 1,1,1,3,3,3-hexafluoroisopropanol, and acetic acid were photolyzed in the same manner.

5.4.2 Steady-State Photolysis

A 0.05 x 0.8 mm quartz tube containing 1 mL of a 5 mL solution of **6** (0.01 M) in dried acetonitrile containing methanol (0.05 M) was sealed with a rubber septum. The sample was irradiated for *ca.* five minutes (8-11 Hg lamps), at which time a 0.5 μL aliquot was removed and injected for analysis by GC. The percent conversion of **6** was calculated relative to dodecane. The sample was photolyzed for an additional five minutes, at which time another aliquot was taken. The conversion of the starting material **6** was followed in this manner to *ca.* 65%.

5.4.3 Competitive Steady-State Photolysis

A 0.05 x 0.8 mm quartz tube containing 1 mL of a 5 mL acetonitrile solution of **6** (0.01M) containing equimolar amounts of methanol (0.05M) and ethanol (0.05M) was sealed with a rubber septum. The sample was irradiated for five minutes (8 Hg lamps) to a conversion of *ca.* 15% of **6** at which time a 0.5 μL aliquot was removed by use of a 10 μL syringe and analyzed by both GC and GC/MS.

5.5 Nanosecond Laser Flash Photolysis

Nanosecond laser flash photolysis experiments employed the pulses from a Lumonics 510 excimer laser filled with F_2/Kr/He mixtures (248 nm, *ca.* 16 ns) and a microcomputer controlled detection system.[93,94] Solutions of 1,1-diphenylsilacyclobutane (**6**) were prepared at concentrations such that the absorbance at the excitation wavelength (248 nm) was *ca.* 0.7-0.8 (10^{-4} - 10^{-3}M), and were flowed continuously from a calibrated 100 mL

capacity reservoir through a 3 x 7 mm Suprasil flow cell. The solutions were oxygenated continuously with a stream of *extra dry* oxygen. Quenchers were added directly to the reservoir by microlitre syringe as aliquots of standard solutions. Quenching rate constants were calculated by linear (eq.1.20; page 21) least squares analysis of decay rate (k_{decay}) versus quencher concentration data which spanned at least one order of magnitude in the transient decay rate.

REFERENCES

(1) Schlenk, W. *Ann.* **1912**, *394*, 221.

(2) Kipping, F. S. *J. Chem. Soc.* **1927**, 104.

(3) Kipping, F. S.; Murray, A. G.; Maltby, J. G. *J. Chem. Soc.* **1929**, 1108.

(4) Pitzer, K. S. *J. Am. Chem. Soc.* **1948**, *70*, 2140.

(5) Mulliken, R. S. *J. Am. Chem. Soc.* **1950**, *72*, 4493.

(6) Dasent, W. E. *Nonexistent Compounds*, Marcel Dekker: New York, 1965; Chapter 4.

(7) Ebsworth, E. A. V. In *Organometallic Compounds of the Group IV Elements*; MacDiarmid, A. G., Eds., Marcel Dekker: New York, 1968; pp 1-89.

(8) Attridge, C. J. *Organomet. Chem. Rev., A*, **1970**, 5, 323.

(9) Gusel'nikov, L. E.; Flowers, M. *J. Chem. Soc., Chem. Commun.* **1967**, 864.

(10) Gusel'nikov, L. E.; Nametkin, N. S.; Vdovin, V. M. *Acc. Chem. Res.* **1975**, *8*, 18.

(11) Gusel'nikov, L. E.; Nametkin, N. S. *Chem. Rev.* **1979**, *79* 529.

(12) Barton, T. J.; McIntosh, C. L. *J. Chem. Soc., Chem. Commun.* **1972**, 861.

(13) Barton, T. J.; Kline, E. A. *J. Organomet. Chem.* **1972**, *42*, C21.

(14) Barton, T. J. *Pure Appl. Chem.* **1980**, *52*, 615.

(15) Coleman, B.; Jones, M. *Rev. Chem. Intermed.* **1981**, *4*, 297.

(16) Wiberg, N. *J. Organomet. Chem.* **1984**, *273*, 141.

(17) Raabe, G.; Michl, J. *Chem. Rev.* **1985**, *85*, 419.

(18) Brook, A. G.; Baines, K. M. *Adv. Organomet. Chem.* **1986**, *25*, 1.

(19) Steinmetz, M. G. *Chem. Rev.* **1995**, *95*, 1527-1588.

(20) Brook, A. G. In *The Chemistry of Organic Silicon Compounds*; Patai, S., Rappoport, Z., Eds.; John Wiley & Sons: New York, 1989; pp 965-1005.

(21) Corey, J.Y. In *The Chemistry of Organic Silicon Compounds*; Rappoport, Z., Patai, S., Eds.; John Wiley & Sons: New York, 1989; pp 1-56.

(22) Nametkin, N. S.; Vdovin, V. M.; Gusel'nikov, L. E.; Zav'yalov, V. I. *Akad. Nauk SSSR, Ser. Khim.* **1966**, 584.

(23) Gusel'nikov, L. E.; Flowers, M. C. *J. Chem. Soc. B*, **1968**, 419.

(24) Schaefer, H. F. *Acc. Chem. Res.* **1982**, *15*, 283.

(25) Trinquier, G.; Malrieu, J. P. *J. Am. Chem. Soc.* **1982**, *104*, 6313.

(26) Wiberg, N.; Wagner, G.; Muller, G.; Riede, J. *J. Organomet. Chem.* **1984**, *271*, 381.

(27) Wiberg, N.; Wagner, G.; Muller, G. *Angew. Chem., Int. Ed. Engl.* **1985**, *24*, 229.

(28) Gordon, M. S. *J. Am. Chem. Soc.* **1982**, *104*, 4352.

(29) Apeloig, Y.; Karni, M. *J. Am. Chem. Soc.* **1984**, *106*, 6676.

(30) Apeloig, Y.; Karni, M. *J. Chem. Soc., Chem. Commun.* **1984**, 768.

(31) Schmidt, M. W.; Gordon, M.S.; Dupuis, M. *J. Am. Chem. Soc.* **1985**, *107*, 2585.

(32) Gordon, M. S.; Koob, R. D. *J. Am. Chem. Soc.* **1981**, *103*, 2939.

(33) Hanamura, M.; Nagase, S.; Morokuma, A. *Tetrahedron Lett.* **1981**, *22*, 1813.

(34) Hood. D. M.; Shaefer, H. F. *J. Chem. Phys.* **1978**, *68*, 2985.

(35) Curtis, M. D. *J. Organomet. Chem.* **1973**, *60*, 63.

(36) Damrauer, R.; Williams, D. R. *J. Organomet. Chem.* **1974**, *66*, 241.

(37) Blustin, P. H. *J. Organomet. Chem.* **1976**, *105*, 161.

(38) Colvin, E. W. *Silicon in Organic Synthesis*; Butterworths Monographs in Chemistry and Chemical Engineering: Butterworth and Co (Publishers) Ltd, 1981; pp 4-10.

(39) Rosmus, P.; Bock, H.; Solouki, B.; Maier, G.; Mihm, G. *Angew. Chem., Int. Ed. Engl.* **1981**, *20*, 598.

(40) Janoschek, R. In *Organosilicon Chemistry From Molecules to Materials*; Auner, N.; Weis, J., Eds.; Verlagsgesellschaft: Weinheim, Germany, 1994; pp 81-86.

(41) Sadtler Index of Ultraviolet Spectra, Sadtler Research Laboratories, Division of Bio-Rad Laboratories, 1980.

(42) Maier, G.; Mihm, G.; Reisenauer, H. P. *Angew. Chem., Int. Ed. Engl.* **1981**, *20*, 597.

(43) Maier, G.; Mihm, G.; Reisenauer, H. P. *Chem. Ber.* **1984**, *117*, 2351.

(44) Boudjouk, P.; Sommer, L. H. *J. Chem Soc., Chem. Commun.* **1973**, 54.

(45) Boudjouk, P.; Roberts, J. R.; Golino, C. M.; Sommer, L. H. *J. Am. Chem. Soc.* **1972**, *94*, 7926.

(46) Elsheikh, M.; Pearson, N. R.; Sommer, L. H. *J. Am. Chem. Soc.* **1979**, *101*, 2491.

(47) Bertrand, G.; Dubac, J.; Mazerolles, P.; Ancelle, J. *J. Chem. Soc., Chem. Commun.* **1980**, 382.

(48) Bertrand, G.; Dubac, J.; Mazerolles, P.; Ancelle, J. *Nouv. J. Chim.* **1982**, *6*, 381.

(49) Low, H. C.; John, P. *J. Organomet. Chem.* **1980**, *201*, 363.

(50) Jutzi, P.; Langer, P. *J. Organomet. Chem.* **1980**, *202*, 401.

(51) Bastian, E.; Potzinger, P.; Rotter, A.; Schuchmann, H. P.; von Sonntag, C.; Weddle, G. *Ber. Bunsenges. Phys. Chem.* **1980**, *84*, 56.

(52) Ishikawa, M.; Nakagawa, K. I.; Enokida, R.; Kumada, M. *J. Organomet. Chem.* **1980**, *201*, 155.

(53) Bertrand, G.; Manuel, G.; Mazerolles, P.; Trinquier, G. *Tetrahedron* **1981**, *37*, 2875.

(54) Ishikawa, M.; Fuchikami, T.; Kumada, M. *J. Organomet. Chem.* **1976**, *118*, 155.

(55) Sakurai, H. In *Silicon Chemistry*; Corey, J. Y.; Corey, E.Y.; Gaspar, P. P.,Eds.; Ellis Horwood; Chichester, 1988; pp 163-172.

(56) Sakurai, H. *J. Organomet. Chem.* **1980**, *200*, 261.

(57) Shizuka, H.; Hiratsuka, H. *Res. Chem. Intermed.* **1992**, *18*, 131.

(58) Ishikawa, M. *Pure Appl. Chem.* **1978**, *50*, 11.

(59) Ishikawa, M.; Kumada, M. *Adv. Organomet. Chem.* **1981**, *19*, 51.

(60) Chapman, O. L.; Chang, C. C.; Kolc, J.; Jung, M. E.; Lowe, J. A.; Barton, T. J.; Tumey, M. L. *J. Am. Chem. Soc.* **1976**, *98*, 7844.

(61) Chefekel, M.R.; Skoglund, M.; Kreeger, R. L.; Shechter, H. *J. Am. Chem. Soc.* **1976**, *98*, 7846.

(62) Mal'tsev, A. K.; Khabashesku, V. N.; Nefedov, O. M. *Izv. Akad. Nauk. SSSR ,Ser. Khim.* **1976**, 1193.

(63) Nefedov, O. M.; Mal'stev, A. K.; Khabashesku, V. N.; Korolev, V. A. *J. Organomet. Chem.* **1980**, *201*, 123.

(64) Gusel'nikov, L. E.; Volkova, V. V.; Avakyan, V. G.; Nametkin, N. S. *J. Organomet. Chem.* **1980**, *201*, 137.

(65) Avakyan, V. G.; Gusel'nikov, L. E.; Volkova, V. V.; Nametkin, N. S. *Dokl. Akad. Nauk. SSSR* **1980**, *254*, 657.

(66) Arrington, C. A.; Klingensmith, K. A.; West, R.; Michl, J. *J. Am. Chem. Soc.* **1984**, *106*, 525.

(67) Maier, G.; Mihm, G.; Reisenauer, H.P. *Angew. Chem.* **1981**, *93*, 615.

(68) Auner, N.; Grobe, J. *Anorg. Allg. Chem.* **1979**, *459*, 15.

(69) Baskir, E. G.; Mal'tsev, A. K.; Nefedov, O. M. *Izv. Akad. Nauk. SSSR, Ser. Khim.* **1983**, 1314.

(70) Brook, A. G.; Harris, J. W.; Lennon, J.; El Sheikh, M. *J. Am. Chem. Soc.* **1979**, *101*, 83.

(71) Brook, A. G.; Kallury, R. K. M. R.; Poon, Y. C. *Organometallics* **1982**, *1*, 987.

(72) Brook, A. G.; Nyburg, S. C.; Reynolds, W. F.; Poon, Y. C.; Chang, Y.; Lee, J S.; *J. Am. Chem. Soc.* **1979**, *101*, 6750.

(73) Brook, A. G.; Nyburg, S. C.; Abdesaken, F.; Gutekunst, B.; Gutekunst, G.; Kallury, P. K. M. R.; Poon, Y. C.; Chang, Y.; Wong-Ng, W. *J. Am. Chem. Soc.* **1982**, *104*, 5667.

(74) Brook, A. G.; Safa, K. D.; Lickiss, P. D.; Baines, K. M. *J. Am. Chem. Soc.* **1985**, *107*, 4338.

(75) Shizuka, H; Okazaki, K.; Tanaka, M.; Ishikawa, M.; Sumitani, M.; Yoshihara, K. *Chem. Phys. Lett.* **1985**, *113*, 89.

(76) Gaspar, P. P.; Holten, D.; Konieczny, S.; Corey, J. Y. *Acc. Chem. Res.* **1987**, *20*, 329.

(77) Leigh, W. J.; Sluggett, G. W. *J. Am. Chem. Soc.* **1992**, *114*, 1195.

(78) Leigh, W. J.; Sluggett, G. W. *Organometallics* **1992**, *11*, 3731.

(79) Leigh, W. J.; Sluggett, G. W. *J. Am. Chem. Soc.* **1993**, *115*, 7531.

(80) Sluggett, G. W. Ph.D. Thesis, McMaster University, 1993.

(81) Sluggett, G.W.; Leigh, W. J. *Organometallics* **1994**, *13*, 269.

(82) Leigh, W.J.; Sluggett, G.W. *Organometallics* **1994**, *13*, 1005.

(83) Leigh, W.J.; Sluggett, G.W. *J. Am. Chem. Soc.* **1994**, *116*, 10468.

(84) Banisch, J. H. Bsc. Thesis, McMaster University, 1992.

(85) Leigh, W. J.; Banisch, J. H. unpublished results.

(86) Leigh, W. J.; Bradaric, C. J.; Sluggett, G. W. *J. Am. Chem. Soc.* **1993**, *115*, 5332.

(87) Jones, P. R.; Bates, T. F. *J. Am. Chem. Soc.* **1987**, *109*, 913.

(88) Kira, M.; Maruyama, T.; Sakuari, H. *J. Am. Chem. Soc.* **1991**, *113*, 3986.

(89) Fink, M. J.; Puranik, D. B.; Johnson, M. P. *J. Am. Chem. Soc.* **1988**, *110*, 1315.

(90) Puranik, D. B.; Fink, M. J. *J. Am. Chem. Soc.* **1989**, *111*, 5951.

(91) Vollhardt, K. P. C. *Organic Chemistry*; W.H. Freeman, and Company: New York, 1987.

(92) Gillom, R. D. *Introduction to Physical Organic Chemistry;* Addison-Wesley Publishing Company: Philipines, 1970.

(93) Hadel, L.M. In CRC Handbook of Organic Photochemistry, Vol. I, Scaiano, J. C., Ed.; CRC Press; Boca Raton, FL, 1989; pp 279-292.

(94) Scaiano, J. C. In CRC Handbook of Organic Photochemistry, Vol. II, Scaiano, J. C., Ed.; CRC Press; Boca Raton, FL, 1989; pp 343-346.

(95) Davidson, M. T.; Dean, C. E.; Lawrence, F. T. *J. Chem. Soc., Chem. Commun.* **1981**, 52.

(96) Nagase, S.; Kudo, T. *J. Chem. Soc., Chem. Commun.* **1983**, 363.

(97) Nagase, S.; Kudo, T.; Ito, K. In *Applied Quantum Chemistry*; Smith, V. H.; Schaefer, H. F., Eds.; D. Reidel Publishing Company: Dordrecht, Holland, 1986; pp. 249-267.

(98) Auner, N.; Grobe, J. *J. Organomet. Chem.* **1980**, *188*, 25-52.

(99) Brook, A. G.; Dillon, P. J. *Can. J. Chem.* **1969**, *47*, 4347.

(99a) Horner, L.; Mathias, J. *J. Organomet. Chem.* **1985**, *282(2)*, 155.

(99b) Lukevics, E.; Pudova, O. A.; Dzintara, M. *Zh. Obshch. Khim.* **1984**, *54(2)*, 339.

(99c) Markov, B. A.; Rybkina, T. I.; Kirichenko, E. A.; Kopylov, V. M.; Prikhod'ko, P. L. *Deposited Doc.* **1980**, VINITI 4276.

(99d) Payne, N. C.; Stephan, D. W. *Inorg. Chem.* **1982**, *21(1)*, 182.

(100) Aldrich, *Catalog Handbook of Fine Chemicals*, Aldrich Chemical Company, 1988.

(101) Silverstein, R. M. *Spectrometric Identification of Organic Compounds*, John Wiley & Sons: New York, 1981; pp 322.

(102) Turro, N. J. *Modern Molecular Photochemistry*; Bejamin/Cummings: Menlo Park, 1978.

(103) Riddick, J. A.; Bunger, W. B.; Sakano, T. K. *Organic Solvents. Physical Properties and Methods of Purification*, **1986**, Vol. II, John Wiley & Sons, New York.

(104) Carey, F. A.; Sundberg, R. J. *Advanced Organic Chemistry*; Plenum Press: New York, 1990.

(105) Hine, J. *Physical Organic Chemistry*, McGraw-Hill, New York, 1962.

(106) Leigh, W. J.; Bradaric, C. J. unpublished results.

(107) Atkins, P. W. Physical Chemisrty, W. H. Freeman and Company, New York, 1986; pp 730.